THE UNIVERSITY OF ALBERTA

ANALYSIS OF SERIES EXPANSIONS

IN LATTICE STATISTICS

by

© JOHN REGINALD LOTHIAN

A THESIS

SUBMITTED TO THE FACULTY OF GRADUATE STUDIES AND RESEARCH

IN PARTIAL FULFILLMENT OF THE REQUIREMENTS FOR THE DEGREE

OF MASTER OF SCIENCE

DEPARTMENT OF PHYSICS

EDMONTON, ALBERTA

FALL, 1972

UNIVERSITY OF ALBERTA

FACULTY OF GRADUATE STUDIES AND RESEARCH

The undersigned certify that they have read, and recommend to the Faculty of Graduate Studies and Research for acceptance, a thesis entitled ANALYSIS OF SERIES EXPANSIONS IN LATTICE STATISTICS, submitted by John Reginald Lothian in partial fulfillment of the requirements for the degree of Master of Science.

ABSTRACT

PART I

The exact high temperature series expansions for the Ising model specific heat are studied using series analysis techniques. The estimates for the critical exponent α from the series on the face-center cubic, body-center cubic, and simple cubic lattices are found to converge and the analysis indicates that the critical exponent of the Ising model specific heat is $\alpha = 0.114$. This value is in disagreement with the present accepted value of $\alpha = 1/8$.

The exact high temperature series expansion for the XY model specific heat on the face-center cubic lattice is analyzed. The analysis of the specific heat series and its derivative is found to be consistent with a specific heat index of $\alpha = 0$, corresponding to a logarithmic singularity. A functional form for the XY model specific heat, which is consistent with the analysis, is presented.

The estimates of the critical exponent for the specific heats of the Ising and XY models are compared with experiment. A good agreement with experimental systems is found for both models.

PART II

A new test of scaling theory in the critical region is proposed. The low temperature series expansions for the two and three dimensional Ising model magnetization on critical paths of the form $(T_c - T)/T_c \propto H^p$ is studied using series analysis techniques and the estimates of the critical exponent on these paths is compared with the predictions of scaling theory. A good agreement with scaling theory is found in both two and three dimensions.

ACKNOWLEDGEMENTS

I would like to thank my supervisor, Dr. D.D. Betts, who suggested the topics on which this thesis is based, for his constant help and guidance.

I am grateful to Dr. C.J. Elliott for his many helpful discussion and assistance with the computer programming. I would also like to thank Dr. J. Stephenson for his advice and assistance.

I am very grateful to Mrs. Mary Yiu for the excellent and speedy manner in which she typed the manuscript.

I would like to thank the Department of Physics for financial support during the past two years.

Finally, I would like to thank my wife Marian whose patience and encouragement made a difficult task less so.

TABLE OF CONTENTS

TABLES

TABLES

TABLES

TABLES

FIGURES

FIGURES

PART I

SPECIFIC HEAT SERIES

CHAPTER 1

HIGH TEMPERATURE EXPANSION OF THE ISING MODEL

SPECIFIC HEAT FUNCTION

In this chapter a brief review of some of the standard techniques used to derive high temperature series expansions is presented. A thorough review of the various methods of deriving high temperature series expansions for the Ising model has been given by Domb (1960). It is not the intention of the author to give a lengthy review of the concepts of graph theory, which is widely used in deriving the high temperature series expansions. For a greater insight into such concepts, the reader is referred to Domb (1960) or Sykes, Essam, Heap, and Hiley (1966).

The Hamiltonian of the spin one-half Ising model with nearest neighbor interactions may be written in the form (Domb 1960)

$$H = - J \sum_{<i,j>} \sigma_i \sigma_j - m H \sum_{i=1}^{N} \sigma_i \tag{1.1}$$

where $\sigma_i = \pm 1$ is the spin variable associated with the i^{th} site on the lattice, m is the magnetic moment, H the external field, J is the interaction energy between neighboring sites, and N is the number of sites on the lattice. The σ variables take the values ± 1 according to whether the magnetic moment is parallel or anti-parallel to the magnetic field.

The thermodynamics of the Ising model are computed from the partition function, which from the

Hamiltonian (1.1) takes the form

$$Z_N = \sum_{\sigma_1=\pm1,\ldots\sigma_N=\pm1} \exp[(J/kT) \sum_{<i,j>} \sigma_i\sigma_j + mH/kT \sum_{i=1}^{N} \sigma_i] \tag{1.2}$$

where the outermost sum is over the 2^N possible values of σ_i for the N lattice sites.

Since the σ variables commute (1.2) can be written as a product

$$Z_N = \prod_{<i,j>} \exp K(\sigma_i\sigma_j) \prod_{i=1}^{N} \exp(L\,\sigma_i) \tag{1.3}$$

where $K = J/kT$ and $L = mH/kT$. The $\sigma_i\sigma_j$ satisfy the relations

$$(\sigma_i\sigma_j)^2 = (\sigma_i\sigma_j)^4 = \ldots = 1, \quad (\sigma_i\sigma_j) = (\sigma_i\sigma_j)^3 = (\sigma_i\sigma_j)^5 = \ldots . \tag{1.4}$$

and hence

$$\exp(K\sigma_i\sigma_j) = \cosh K + \sigma_i\sigma_j \sinh K \quad . \tag{1.5}$$

The first product in (1.3) can be expanded as follows (van der Waerden 1941)

$$\prod_{<i,j>} (\cosh K + \sigma_i\sigma_j \sinh K) = \cosh^{qN/2} K \prod_{<i,j>} (1 + \sigma_i\sigma_j \tanh K)$$

$$= (\cosh K)^{qN/2} [1 + (\tanh K) \sum_{<i,j>} \sigma_i\sigma_j$$

$$+ (\tanh K)^2 \sum_{<i,j><k,\ell>} \sigma_i\sigma_j\sigma_k\sigma_\ell + \ldots] \tag{1.6}$$

where $qN/2$ is the number of nearest neighbor bonds in the lattice. When H is set equal to zero the second factor in (1.3) becomes unity and the zero field partition function is simply written as

$$Z_N = (\cosh K)^{qN/2} \sum_{\sigma_1=\pm 1, \ldots, \sigma_N=\pm 1} [1 + \tanh K \sum_{\langle i,j \rangle} \sigma_i \sigma_j$$

$$+ \tanh^2 K \sum_{\langle i,j \rangle \langle k,\ell \rangle} \sigma_i \sigma_j \sigma_k \sigma_\ell + \ldots] \qquad (1.7)$$

A graph theoretical interpretation of (1.7) can now be given. With each $(\sigma_i \sigma_j)$ one associates a nearest neighbor bond (an edge of a graph) of the lattice and any configuration with an odd number of edges meeting at a vertex will have an odd σ_i left in the summation, and will give zero contribution. Hence the only non-zero contribution arises from closed graphs, each vertex of which is the meeting point of an even number of edges or in the terminology of graph theory the vertex is of even degree. Thus with each term of (1.7) one can associate one graph, whose vertices are all of even degree. Such graphs, connected and separated, are called no-field graphs.

The partition function (1.7) can now be written as

$$Z_N = 2^N (\cosh K)^{qN/2} [1 + \sum_{r=1}^{qN/2} p(r) \tanh^r K] \quad . \qquad (1.8)$$

where $p(r)$ denotes the total number of ways of embedding in the lattice all graphs of r edges whose vertices are all of even degree. The $p(r)$ are in general polynomials of degree r in N. Any such graph gives a contribution of 2 for each vertex when the sum over the appropriate σ_i is done. Hence the 2^N in (1.8) arises when one performs the sum over all states.

Instead of (1.8) what one is really interested in is the dimensionless Helmholtz free energy per site defined as

$$-\frac{F}{kT} = \lim_{N\to\infty} \{\log Z_N\}/N \quad . \tag{1.9}$$

Hence

$$-\frac{F}{kT} = \log 2 + (q/2)\log(\cosh K)$$

$$+ \lim_{N\to\infty}\{\log[1 + \sum_{r=1}^{qN/2} p(r)v^r]\}/N \tag{1.10}$$

where $v = \tanh K$. It has been shown by Domb (1960) that

$$\lim_{N\to\infty} \{\log [1 + \sum_{r=1}^{qN/2} p(r)\, v^r]\}$$

corresponds to taking the terms linear in N in the partition function. Thus denoting p_r^1 as the coefficient of the term linear in N in $p(r)$,

$$-\frac{F}{kT} = \log 2 + (q/2)\log(\cosh K)$$

$$+ \sum_{r=1}^{qN/2} p_r^1\, v^r \tag{1.11}$$

The zero field specific heat per site can be obtained from (1.11) by differentiating twice with respect to the temperature, i.e.

$$C_H/kT = \frac{\partial^2}{\partial T^2}\,(-F/k) \quad . \tag{1.12}$$

CHAPTER 2

SERIES ANALYSIS TECHNIQUES

2.1 Critical Exponents

In theoretical and experimental results one usually assumes that the thermodynamic variables have a simple power law behavior near the critical point of a ferromagnetic system (or analogous systems). Therefore near the critical point it is assumed that the thermodynamic function, f(x), of interest is of the form

$$f(x) \sim A(x - x_c)^{\gamma} \qquad (x \to x_c) \qquad (2.1)$$

where x_c is the critical point, γ the critical exponent and A is the critical amplitude.

A precise and general definition of a critical exponent to describe the behavior near the critical point of a general function f(x) is given by

$$\gamma = \lim_{x \to x_c} \frac{\log f(x)}{\log(x-x_c)} \qquad (2.2)$$

where f(x) and $(x-x_c)$ are positive. Of course the existence of the exponent γ does not mean f(x) is simply proportional to $(x-x_c)^{\gamma}$. One must always expect correction terms of higher order, since (2.1) represents only the dominant asymptotic behavior.

For a complete definition of all critical exponents, including those used by the author, the reader is referred to Fisher (1967).

2.2 Ratio Method

The ratio method for analyzing series expansions has been used first by Domb and Sykes (1957a and b) to estimate critical points and exponents. The method has been reviewed by Fisher (1967) and more recently by Gaunt and Guttmann (1973).

If the dominant singularity of a function occurs at some value x_c and is of the form (2.1) then the coefficients a_n in the expansion

$$f(x) = \sum_{n=0}^{\infty} a_n x^n$$

will tend in the limit of large n to the binomial coefficients in the expansion of (2.1). The ratios μ_n of the successive coefficients a_n and a_{n-1} will then tend to

$$\mu_n = \frac{a_n}{a_{n-1}} \sim (1 - \frac{[\gamma + 1]}{n}) \mu_c \qquad (2.3)$$

where $\mu_c = x_c^{-1}$. If the successive values of μ_n are plotted against $1/n$, the location of the singularity can be estimated by extrapolating to the intercept $n = \infty$. The value of γ can be estimated from the limiting slope of the plot. If x_c has been determined by this or any other means a sequence $\gamma(n)$ of estimates

for γ can be formed by rearranging (2.3) as

$$\gamma(n) = n(1 - \mu_n x_c) - 1 \quad . \tag{2.4}$$

To aid the extrapolation of the sequence $\gamma(n)$ one often plots these values against $1/n$ and extrapolates to the intercept $n = \infty$ to get an estimate of γ.

In general the series expansion for $f(x)$ exhibits non-physical singularities as well as physical ones. The physical singularity is usually the closest singularity to the origin on the positive real axis. When there are no non-physical singularities nearer to the origin than the physical singularity the ratios are all positive and when the non-physical singularities lie well outside the circle of convergence defined by the physical singularity, then the ratios will converge rapidly. If the dominant singularity lies on the negative real axis the signs of the series coefficients will alternate and when the dominant singularities are complex, the signs will be irregular. For these cases, different techniques must be employed. It should also be mentioned that more complex singularities may arise such as

$$f(x) \sim A(x - x_c)^{-\lambda} |\ell n(x - x_c)|^{\mu} \quad . \tag{2.5}$$

If (2.5) occurs (2.3) still holds but convergence may be extremely slow.

The ratio method has proved most useful when applied to high temperature Ising model susceptibility series, since in these cases the dominant singularity is on the positive real axis. The low temperature series presented in Chapter 4 does not in general fall into this category, due to the presence of complex pairs of singularities symmetric about the negative real axis and nearer the origin than the physical singularity.

2.3 Transformations of Expansion Variables

It is possible, however, in some cases to transform the physical singularity nearer to the origin than the complex singularities. This is accomplished by transforming the series expansion variable. A conformal transformation of the form

$$x = \frac{ax'}{1 - bx'} \qquad (2.6)$$

is the type of transformation most often used.

Wortis (1969) applied a transformation of this form to the antiferromagnetic susceptibility series of the Ising model on the f.c.c. lattice. After thus transforming the Curie point to infinity the resulting series was successfully analyzed by the ratio method.

More general non conformal transformations can also be used. Betts, Elliott, and Ditzian (1971) introduced a non conformal transformation of the form

$$x = \frac{ax'}{1 - b(x')^2} \tag{2.7}$$

and successfully analyzed the triangular lattice fluctuations series with it. In Chapter 4, the results of the use of several transformations of this form are discussed.

A branch point singularity of the form (2.1) can be transformed into a simple pole by taking the logarithmic derivative of the series for f(x).

The form becomes

$$\frac{d}{dx} \log f(x) \sim \frac{\gamma}{x-x_c} \tag{2.8}$$

and a ratio analysis of (2.8) can be used as a test of how well the series is represented by the form (2.1), since from (2.3) the ratios should approach the constant value μ_c. If an estimate of x_c is available a further extension of the transformation (2.8) of the form

$$F(x) = (x-x_c) \frac{d}{dx} \log f(x) \tag{2.9}$$

is possible. If f(x) has the form (2.1) then $F(x_c)$

should converge to γ. If the series expansion of $F(x)$ is sufficiently regular an upper or lower confidence limit can be put on the estimate of the exponent. This can be done by evaluating the truncated series to $F(x)$ at the critical point x_c, using each successive coefficient of the expansion to $F(x)$. If the series is regular, the last value of $F(x_c)$ can be used as an upper or lower confidence limit, depending on whether the sequence of estimates to $F(x_c)$ appear to be converging on γ from above or below. This new technique in series analysis is being put forward by the author and is used in the analysis of several series in Chapter 4.

2.4 Padé Approximant Method

The Padé approximant method, which was first applied to the Ising model by Baker (1961), approximates a function by the ratio of two polynomials. Following the convention of Fisher (1967), the [L,M] Padé approximant to a power series is defined by

$$[L,M] = \frac{P_L(x)}{Q_M(x)} = \frac{p_o + p_1 x + \ldots + p_L x^L}{1 + q_1 x + \ldots + q_M x^M} \qquad (2.10)$$

The coefficients p_o, p_1 ... p_2, q_1, ... q_M are calculated by requiring the expansion of [L,M] to agree exactly with the given power series, $f(x)$, up to the

order $(L+M) = R$, where R is the order of the term at which $f(x)$ is truncated.

The convergence of Padé approximants to $f(x)$ has been studied by Baker, Gammel, and Wills (1961) and Baker (1965, 1968). This problem will not be considered here but their result, that the $[N,N]$ diagonal approximants may be expected to converge to $f(x)$, will be used. Essam and Fisher (1963) also find that the $[N,N+1]$ and $[N,N-1]$ approximants seem to converge just as well and have used them to estimate the function. The nature of Padé approximant is such that it can represent a simple pole in a function exactly, so it is desirable if possible to transform the function being examined so the singularity is of that form. Convergence in the region of such a pole is rapid while in the region of a branch point it is considerably slower.

In order to use the Padé approximant method most effectively for functions of the form (2.1), the series should be transformed using (2.8), a process which converts the singularity into a simple pole.

If an accurate estimate of the critical exponent γ is available, estimates of the critical point can be obtained by forming Padé approximants to

$$[f(x)]^{-1/\gamma} \sim A^{-1/\gamma}(x-x_c)^{-1} \qquad (2.11)$$

which has a simple pole at $x = x_c$.

If an accurate estimate of the critical point is available, the series can be transformed using (2.9) and the Padé approximants to F(x) can be evaluated at the critical point x_c to obtain estimates of the critical index γ.

One can also use the Padé approximant method to calculate estimates of the amplitude. Taking Padé approximants to the function

$$(x-x_c)[f(x)]^{-1/\gamma} = A^{-1/\gamma} \tag{2.12}$$

and evaluating them at the critical point, will give estimates of A.

CHAPTER 3

ANALYSIS OF ISING MODEL SPECIFIC HEAT SERIES

As noted in Chapter 1 series expansions of the specific heat in zero field can be obtained as a series in ascending powers of $K = J/kT$ or $v = \tanh K$. The extrapolations of the critical indices were found to be quite insensitive to a choice between these variables and therefore analysis is presented in the natural variable v only. The critical behavior of the Ising model specific heat expansions has been studied on the face-centered cubic, body-centered cubic, simple cubic (Sykes et al 1972b), hydrogen peroxide, hypertriangular (Leu, Betts and Elliott 1969), diamond (Essam and Sykes 1963), crystobalite (Gibberd 1970), and the octrahedral (Oitmaa and Elliott 1970) lattices.

Since the f.c.c. lattice is the most closely packed of the lattices considered, more "information" about the structure is contained in the earlier coefficients of the f.c.c. expansion. Hence it is expected that the series for the f.c.c. lattice will approach its limiting behavior more rapidly than the series for the other lattices. In the analysis which follows, this lattice will be the one principally considered, since the emphasis is on methods of analysis. However, most of the calculations have been repeated for the other lattices, and where the results are sufficiently good for inferences to be made about the behavior of the series. They

support all conclusions based on the analysis of the f.c.c. lattice.

The ratio method has been discussed in detail in Section 2.2. In the case of the specific heat the assumed limiting behavior is of the form

$$C_H/k \sim A(1 - v/v_c)^{-\alpha} . \qquad (3.1)$$

Equation (2.3) for the limiting behavior of the ratios of successive coefficients of the series becomes

$$\mu_n \sim (1 + \frac{\alpha-1}{n})\, v_c^{-1} \quad . \qquad (3.2)$$

If v_c is fixed an estimate of α can be obtained from the slope of the ratio curve (when plotted against $1/n$), and from the sequence $\gamma(n)$ defined by equation (2.4). To form this sequence the most recent estimate for v_c, based on the high temperature susceptibility expansion (Sykes et al 1972a),is used. This estimate is

$$v_c = 0.101740 \pm 0.000005$$

or (3.3)

$$v_c^{-1} = 9.8290 \pm 0.0005 \quad .$$

The sequence, together with the sequence of ratios μ_n is given in Table 3.1. The sequence $\gamma(n)$ in Table 3.1 seems to be converging to a constant value; for $n = 9 \ldots\ldots 14$ the values of $\gamma(n)$ are very close

Table 3.1

Ratios of the f.c.c. specific heat, together with sequence of estimates $\gamma(n)$ of the critical exponent using the critical point $v_c = 0.10174$.

n	μ_n	$\gamma(n)$
3	8.0000	-0.4418
4	8.2083	-0.3405
5	8.2437	-0.1935
6	8.3458	-0.0946
7	8.5495	-0.0888
8	8.7371	-0.1113
9	8.8717	-0.1235
10	8.9709	-0.1270
11	9.0489	-0.1269
12	9.1130	-0.1259
13	9.1673	-0.1248
14	9.2139	-0.1240

together. The sequence $\gamma(n)$ (solid line) is plotted versus $1/n$ in Figure 3.1. Also shown are similar sequences for the b.c.c. (dotted line) and s.c. (broken line) lattices, which were the only other lattices with regular ratios. For loose packed lattices, such as the b.c.c. and s.c. lattices, only even terms are present in the specific heat expansion and (2.4) must be slightly modified. The modified form is

$$\gamma(n) = n\left(1 - \frac{a_{2n}}{a_{2n-2}} v_c^2\right) - 1 . \qquad (3.4)$$

To form these sequences, the following values of v_c (Sykes et al 1972a) have been used

$$\begin{array}{lll} \text{Simple cubic} & v_c^{-1} = 4.5844 \pm 0.0002 & \\ & & (3.5) \\ \text{Body centered cubic} & v_c^{-1} = 6.4055 \pm 0.0010 . & \end{array}$$

There is a close similarity in the behavior of the three sequences; they seem consistent with the view that α for the Ising model is determined only by the dimensionality of the lattice and not by its detailed structure. They are also consistent with the view that α is very close to 1/8. To obtain a value of $\gamma(14)$ for the face centered cubic of -0.1250 requires $1/v_c = 9.8280$. Thus if the limit is exactly 1/8 the sequences must pass through a minimum.

FIGURE 3.1

ESTIMATES FOR THE CRITICAL INDEX δ FOR THE f.c.c., b.c.c., AND s.c. LATTICES CALCULATED FROM (3.2) AND (3.4)

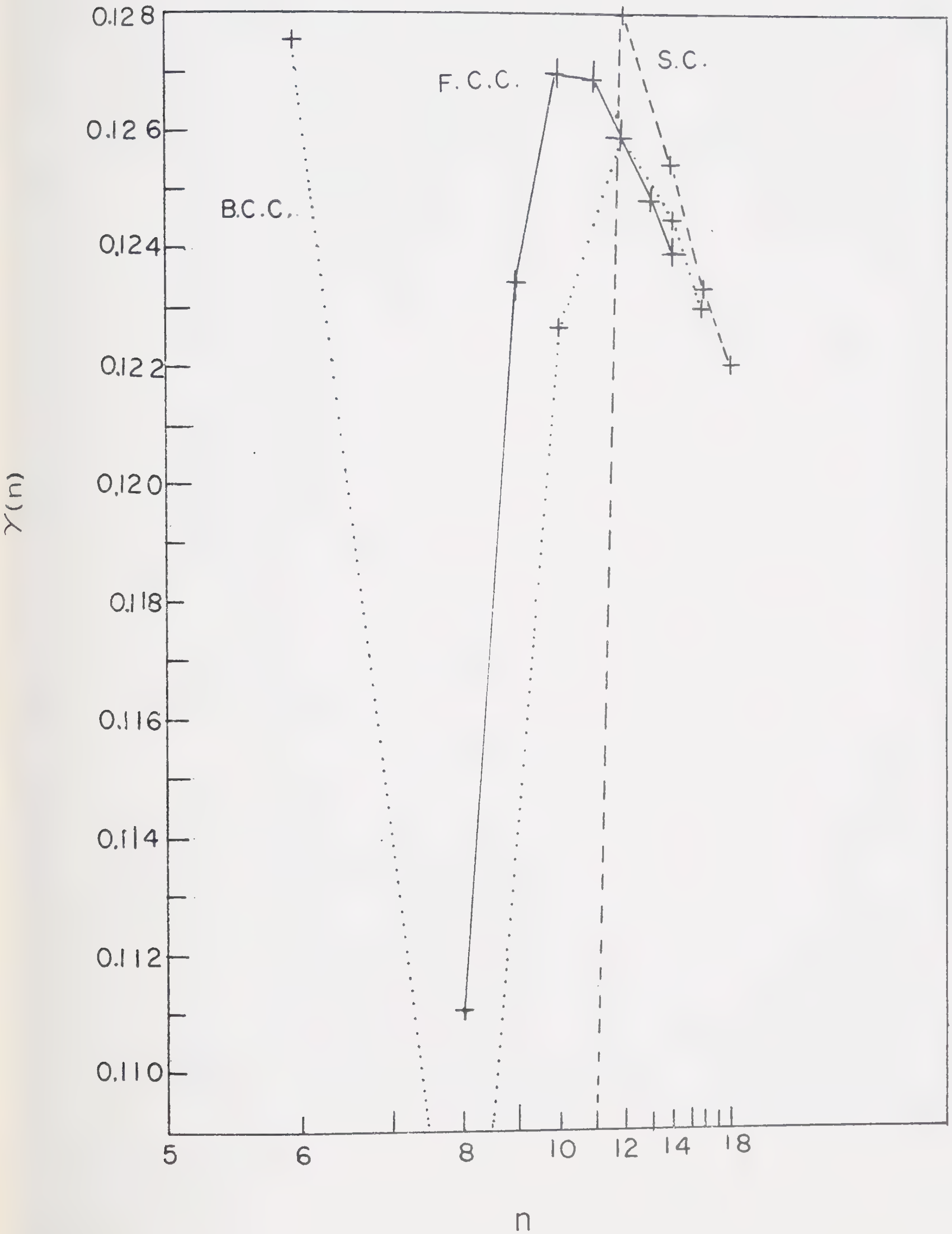
0.128
0.126
0.124
0.122
0.120
0.118
0.116
0.114
0.112
0.110
γ(n)
B.C.C.
F.C.C.
S.C.
5
6
8
10
12
14
18
n

In Figure 3.2 the ratios μ_n for the f.c.c. series are plotted against 1/n in the usual way. In addition in this Figure we have shown two lines (dotted) which have slopes corresponding to $\alpha = 1/8$ and $\alpha = 0$ and which have the intercept $v_c^{-1} = 9.8290$. The last six points of the ratio plot appear to lie on the line corresponding to $\alpha = 1/8$. This is a graphical expression of the fact that the last six values of $\gamma(n)$ are very close to -1/8. It illustrates in a striking fashion how unlikely it would be for the ratios, after having settled down to such regular behavior which points to the known intercept, to indicate subsequently another simple value for α. The ratio method strongly suggests α is very close to an 1/8 on the f.c.c. lattice. The evidence of the b.c.c. and s.c. also tends to support this assumption.

When the Padé approximate methods of Section 2.4 are applied directly to the specific heat series the results are very inconclusive. In Table 3.2 the location of the physical pole and the residue for a few Padé approximants to the logarithmic derivative of the specific heat on the f.c.c. lattice are given. Notice that the Padé approximants have not converged to the critical point as well as the ratio method and also

FIGURE 3.2

RATIOS μ_N VS. 1/n FOR THE ISING MODEL

SPECIFIC HEAT ON THE f.c.c. LATTICE

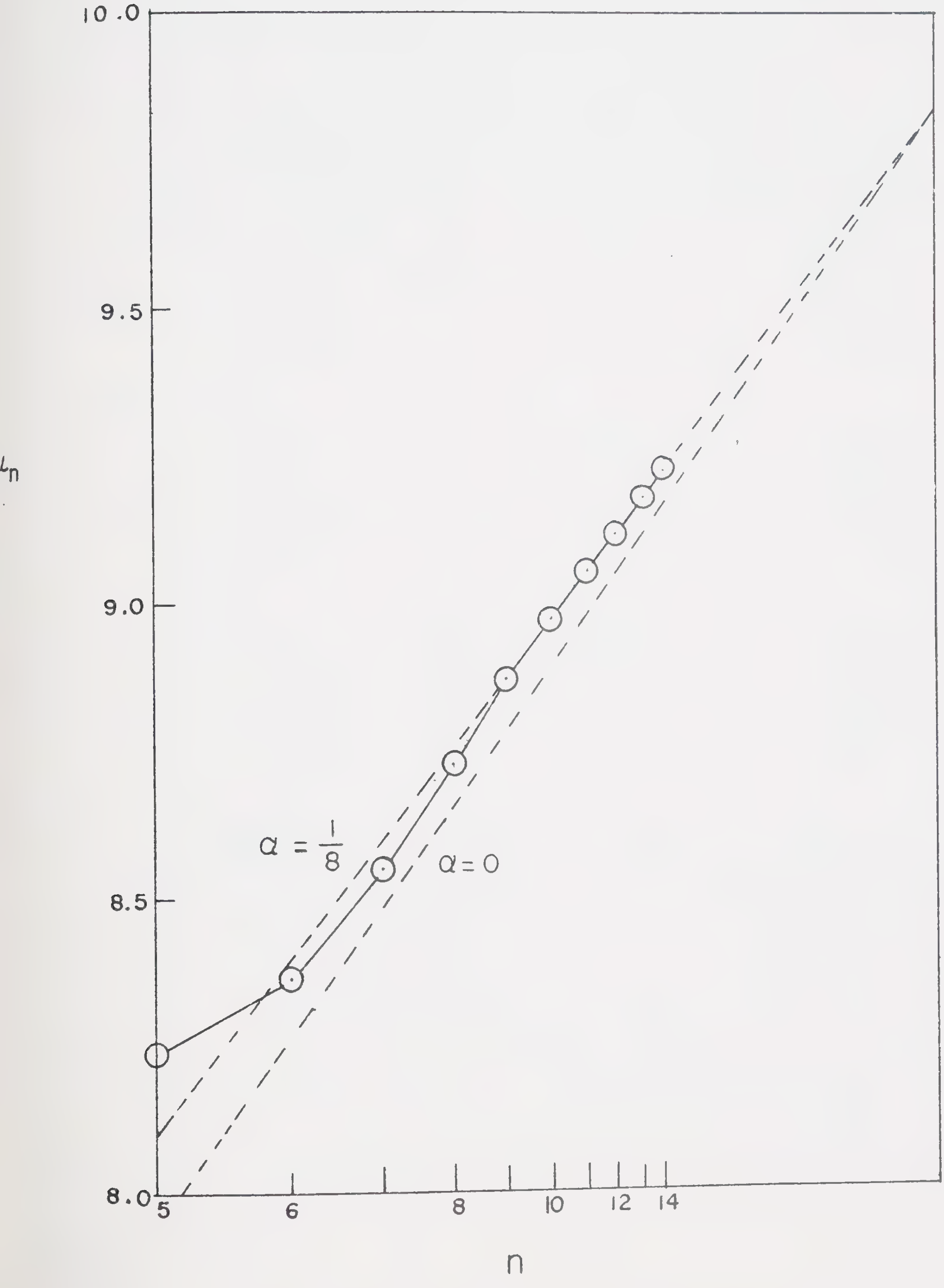

10.0
9.5
9.0
8.5
8.0
ι_n
$\alpha = \frac{1}{8}$
$\alpha = 0$
5
6
8
10
12
14
n

Table 3.2

Estimates of v_c and α from the series expansion for C_H from the location of the poles and the residue of Padé approximants to $d/dv \log(C_H/v^2)$.

Approximant [L,M]	Singularity	Residues
[4,7]	0.10249	0.4225
[5,6]	0.10256	0.4290
[6,5]	0.10264	0.4359
[7,4]	0.10261	0.4329
[4,6]	0.10284	0.4520
[5,5]	0.10215	0.3932
[6,4]	0.10289	0.4575
[7,3]	0.10340	0.4978
[3,6]	0.10356	0.5052
[4,5]	0.10440	0.5526
[5,4]	0.10744	0.5486
[6,3]	0.10465	0.5651
RATIO RESULT	(0.10174)	(0.125)

the critical exponent is not even close to the estimate from the ratio method. Since there is a good estimate of v_c, Pade approximants to the function (2.9) evaluated at $v_c = 0.10174$ will give an estimate of α. These are listed in Table 3.3. Notice that they give $\alpha = 0.35$ in strong contrast to the ratio result. There is also a large spread in the values for both Tables.

Hunter (1968) found that the mimic function

$$C_H/R \sim A\{(1 - v/v_c)^{-\alpha} - 1 - \alpha v/v_c\} \qquad (3.6)$$

best approximated the f.c.c. specific heat series. If this conjecture is right it would explain why direct Padé analysis of the specific heat gives such poor results. The form of the mimic function suggests the second derivative of the specific heat with respect to v is the function to analyze with Padé approximant methods. The first derivative with respect to v should also give better results when analyzed. To test this conjecture Padé approximant analysis similar to that done on C_H is performed on $(d/dv)C_H$ and $(d/dv)^2C_H$. The results are given in Tables 3.4 and 3.5. In Table 3.4 the location of the physical singularity and corresponding estimates of α for the Padé approximants to the logarithmic derivative of both $(d/dv)C_H$ and $(d/dv)^2C_H$ are given. These Padé approximants give

Table 3.3

Estimates of α from evaluating Padé approximants to $(v-v_c)(d/dv)\log(C_H/v^2)$.

Approximant [L,M]	Value
[4,7]	0.3499
[5,6]	0.3463
[6,5]	0.3601
[7,4]	0.3440
[4,6]	0.3542
[5,5]	0.3573
[6,4]	0.3575
[7,3]	0.3555
[3,6]	0.5563
[4,5]	0.3633
[5,4]	0.3589
[6,3]	0.3615
[3,5]	0.3836
[4,4]	0.1925
[5,3]	0.3490
[6,2]	0.7150
RATIO RESULT	(0.125)

Table 3.4

Estimates of v_c and α from series expansions for C_H' and C_H'' from the poles and residues of Pade approximants to g(v).

Approximant [L,M]	$g(v) = \frac{d}{dv} \log(\frac{1}{v} \frac{d}{dv} C_H)$		$g(v) = \frac{d}{dv} \log(\frac{d^2}{dv^2} C_H)$	
	Location of singularity	Estimate of α from residue	Location of singularity	Estimate of α from residue
[4,7]	0.10170	0.1080	0.10177	0.1276
[5,6]	0.10174	0.1136	0.10212	0.2055
[6,5]	0.10174	0.1136	0.10218	0.2191
[7,4]	0.10173	0.1128	0.10218	0.2190
[4,6]	0.10184	0.1274	0.10230	0.2446
[5,5]	0.10173	0.1132	0.10222	0.2261
[6,4]	0.10134	0.1004	0.10215	0.2132
[7,3]	0.10171	0.1103	0.10222	0.2264
[3,6]	0.10036	-0.0016	0.10565	1.428
[4,5]	0.10146	0.0840	0.10199	0.1826
[5,4]	0.10168	0.1070	0.10218	0.2116
[6,3]	0.10168	0.1066	0.10218	0.2175
[3,5]	0.10107	0.0541	0.09454	-0.1382
[4,4]	0.10082	0.0384	0.10300	0.3778
[5,3]	0.10164	0.1026	0.10216	0.2146
[6,2]	0.10183	0.1215	0.10011	-0.1360
RATIO RESULT	(0.10174)	(0.1250)	(0.10174)	(0.1250)

Table 3.5

Estimates of α from series expansions for C_H' and C_H'' based on evaluation of Pade approximants to F(v) at $v = v_c = 0.10174$ for the f.c.c. lattice.

Approximant [L,M]	$F(v)=(v_c-v)\frac{d}{dv} \times \log(\frac{1}{v}\frac{d}{dv}C_H)$	$F(v)=(v-v_c)\frac{d}{dv} \times \log(\frac{d^2}{dv^2}C_H)$
	Value	Value
[4,7]	0.1142	0.1208
[5,6]	0.1141	0.1207
[6,5]	0.1142	0.1075
[7,4]	0.1141	0.3577
[4,6]	0.1138	0.1214
[5,5]	0.1141	0.1452
[6,4]	0.1141	0.2371
[7,3]	0.1140	0.2353
[3,6]	0.1194	0.1865
[4,5]	0.1149	0.1354
[5,4]	0.1140	0.1338
[6,3]	0.1149	0.3950
[3,5]	0.1214	0.1792
[4,4]	0.1095	0.1405
[5,3]	0.1133	0.1478
[6,2]	0.1130	0.1432
RATIO RESULT	(0.125)	(0.125)

results quite consistent with the ratio method. In Table 3.5 evaluations of the Padé approximants to function (2.9) for the $(d/dv)C_H$ and $(d/dv)^2C_H$ are given. Again both give results consistent with the ratio method. From these Tables it is seen that Padé analysis of the first derivative of the specific heat seems to give the most consistent results. This was also true for the other seven Ising models specific heat series analyzed. Table 3.5 gives an estimate of $\alpha = 0.114$ from the analysis of the first derivative. This is very close to the ratio result.

The widely held view that the specific heat of a three dimensional Ising model of a ferromagnet diverges at the critical temperature, from above, inversely as an one eighth power is consistent with the analysis presented here, but the author believes the analysis shows α to be slightly less than 1/8. However the evidence that α is close to 1/8 is strong.

In Figure 3.1 the sequences for $\gamma(n)$ appear to be linear in 1/n for the last few terms. Linearly extrapolating this sequence to $n = \infty$ yields $\gamma(\infty)=0.114$. This is in agreement with Table 3.5. Thus a value of $\alpha = 0.114$ is possibly a "better"choice for α.

CHAPTER 4

ANALYSIS OF THE XY MODEL HIGH TEMPERATURE SPECIFIC HEAT SERIES

This chapter is concerned with the analysis of exact high temperature series expansions of the spin 1/2 XY model of ferromagnetism or of a quantum lattice fluid. This model was originally introduced by Matsubara and Matsuda (1956) as a model of a quantum lattice fluid. The spin 1/2 XY model is of great theoretical interest as probably the simplest quantum mechanical many-body system (excluding "diagonal" models like the Ising model) and it is also of experimental interest as a model of an insulating ferromagnet or antiferromagnet.

Methods for derivations of the expansions will not be given here but the interested reader is referred to Betts, Elliott and Lee (1970) and Betts (1973). Eleven coefficients in the specific heat series for the f.c.c. and b.c.c. lattices have been derived by Betts and his co-workers at the University of Alberta (Betts, Elliott and Lee 1969, 1970 and Betts and Lee 1968). Only the f.c.c. lattice will be studied here since the series on the b.c.c. lattice gave very poor results and no conclusions could be made about the critical behavior of the specific heat on this lattice.

From a ratio analysis of the fluctuation series, Betts, Elliott and Lee (1970) estimated the critical temperature $K_c = J/kT_c$ to be

$$K_c = 0.2210 \pm 0.0006$$

or (4.1)

$$K_c^{-1} = 4.524 \pm 0.013$$

on the f.c.c. lattice. This value of the critical temperature has been accepted as the "best" estimate of the critical point for the specific heat series. As in the case of the Ising model the XY model will be assumed initially to be of the form (2.1).

Figure 4.1 contains a standard ratio plot for the specific heat on the f.c.c. lattice. The ratio of successive coefficients μ_n is plotted versus 1/n. Also shown are two lines (dashed) which have slopes corresponding to $\alpha = 1/4$ and $\alpha = 0$ and which have the intercept $K_c^{-1} = 4.524$. The ratios exhibit a very strong oscillation and very little can be estimated about their limiting behavior.

When the Padé approximants were applied directly to the specific heat the results were very inconclusive. In Table 4.1 estimates of the location of the critical point K_c and the exponent α from the poles and residues respectively of Pade approximants to the logarithmic derivative of the f.c.c. specific heat are given. This Table gives the estimates $K_c =$ 0.235 and $\alpha = 0.6$. This is in strong conflict with

FIGURE 4.1

RATIOS μ_n VS. 1/n FOR THE XY MODEL

SPECIFIC HEAT ON THE f.c.c. LATTICE

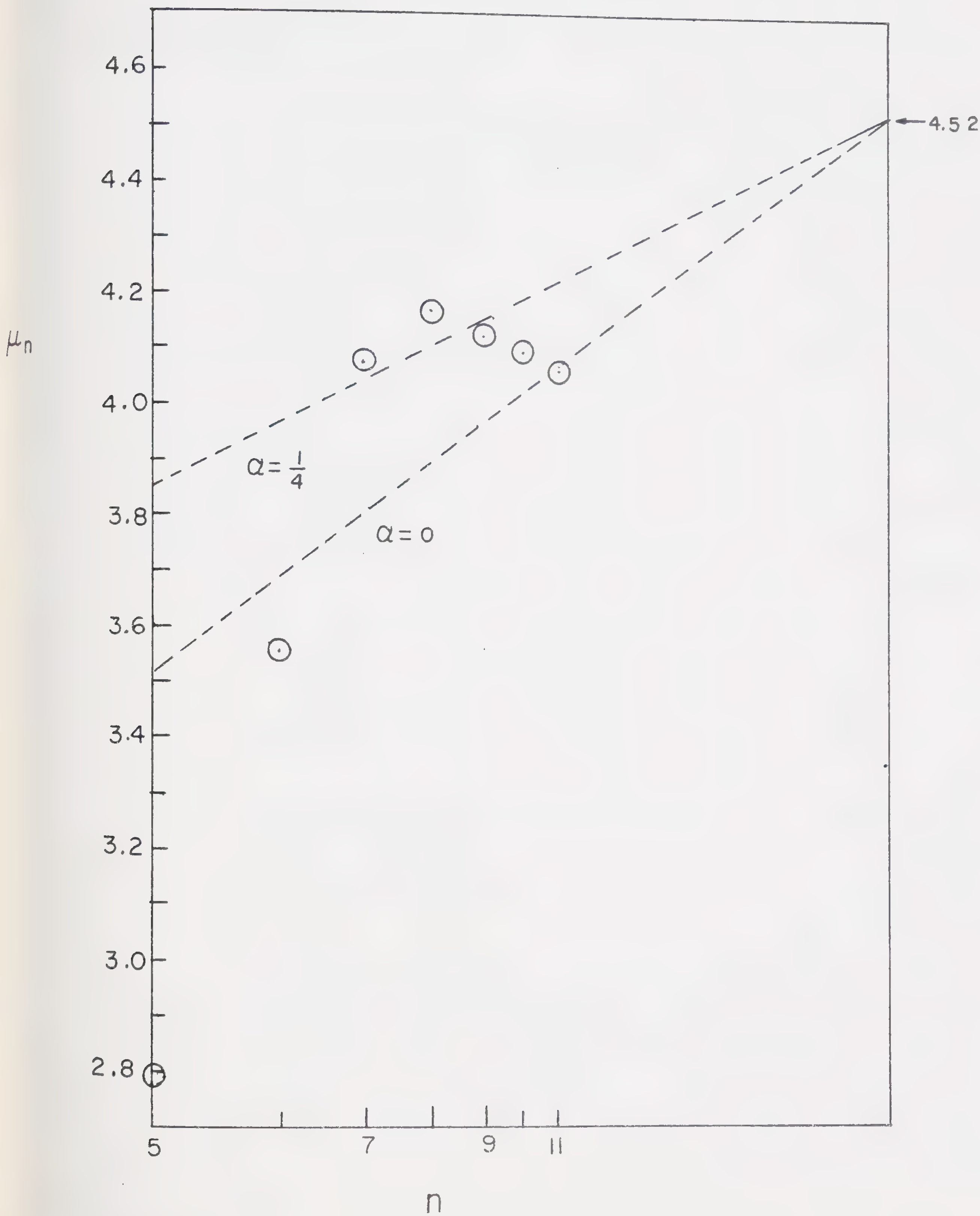
4.6
4.4
4.2
4.0
3.8
3.6
3.4
3.2
3.0
2.8
4.52
μ_n
$\alpha = \frac{1}{4}$
$\alpha = 0$
5
7
9
11
n

Table 4.1

Estimates of K_c and α from Padé approximants to $(d/dK) \log(C_H/K^2)$.

Approximant [L,M]	Singularity	Residue
[3,5]	0.1273	0.001
[4,4]	0.2352	0.602
[5,3]	0.2352	0.603
[6,2]	0.2304	0.503
[2,5]	0.2352	0.599
[3,4]	0.2365	0.635
[4,3]	0.2360	0.622
[5,2]	0.2364	0.633
[2,4]	0.2772	-3.98
[3,3]	0.2351	0.600
[4,2]	0.2352	0.602
[5,1]	0.2274	0.202

$K_c = 0.2210$ from the fluctuation series. Also α is expected to be much smaller than 0.6. When the Padé approximants to function (2.9) are evaluated at $K_c = 0.2210$ to get an estimate of α, a value of $\alpha = 38$ is obtained. This is clearly not a very good estimate, and it indicates that (2.1) may not be a very good choice for the form of the specific heat.

In an effort to improve the ratios several transformations of the form (2.6) and (2.7) have been tried. No Euler transformation improves the ratios but several transformations of the form (2.7) do improve the ratios. The three "best" transformations tried are

$$K = \frac{K'}{1.4[1 - (K')^2]} \tag{4.2}$$

$$K = \frac{K'}{1.5[1 - (K')^2]} \tag{4.3}$$

$$K = \frac{K'}{1.6[1 - (K')^2]} \quad . \tag{4.4}$$

In Figure 4.2 the ratios corresponding to these transformations are plotted versus $1/n$. In order to plot all three on the graph, the ratios are divided by the transformed critical temperature K_c' for each

FIGURE 4.2

RATIOS μ_n VS. $1/n$ FOR THE TRANSFORMED f.c.c. SPECIFIC HEAT USING TRANSFORMATIONS (4.2), (4.3), AND (4.4).

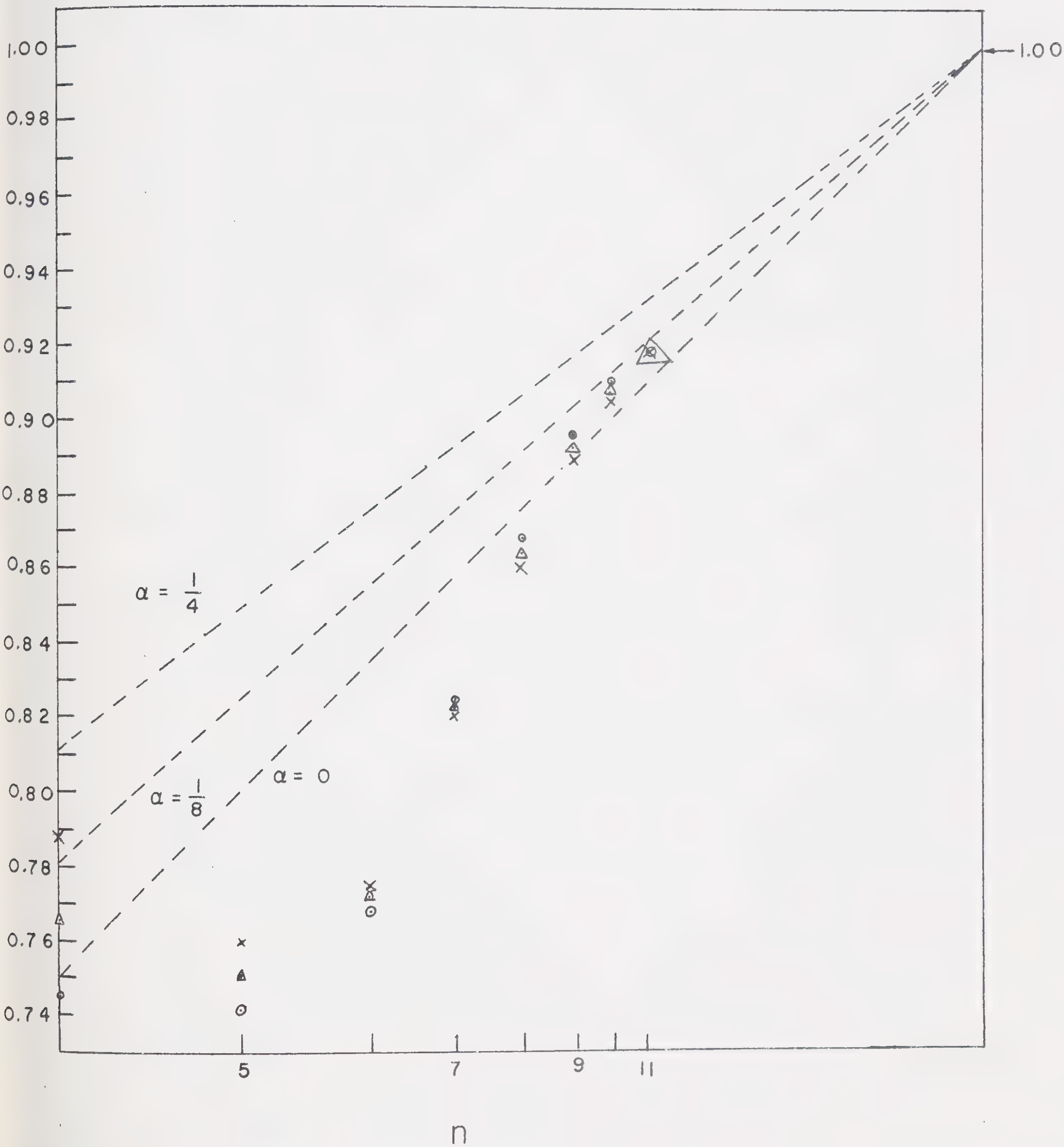

1.00
0.98
0.96
0.94
0.92
0.90
0.88
0.86
0.84
0.82
0.80
0.78
0.76
0.74
1.00
$\alpha = \frac{1}{4}$
$\alpha = \frac{1}{8}$
$\alpha = 0$
5
7
9
11
n

transformation. The circles correspond to $a = 1/1.4$, $b = 1$ and $K_c' = 0.2844$, the triangles to $a = 1/1.5$, $b = 1$ and $K_c' = 0.3014$, and the x's to $a = 1/1.6$, $b = 1$ and $K_c' = 0.3179$. Also shown are three lines (dotted) corresponding to $\alpha = 1/4$, $\alpha = 1/8$, and $\alpha = 0$, and which have the known intercept of unity. Notice that in these ratios the oscillation is still present but considerably damped. A precise estimate of α is not possible, but all three sets of ratios appear to oscillate about a value of $\alpha \leq 1/8$.

Padé approximants to the logarithmic derivative of $(d/dK)C_H$ and $(d/dK)^2 C_H$ do not give a useful estimate of α. These approximants do not locate the physical singularity with any consistency. The Padé approximants to the function (2.9) for $(d/dK)C_H$ and $(d/dK)^2 C_H$ give estimates of α which are clearly in error.

The specific heat series for the XY model seems intractable to the standard Padé approximant techniques. When the ratio plots in Figures (4.1) and (4.2) are re-examined a possible explanation for this failure of the Padé approximant methods is found. The ratios in both Figures seem to oscillate about $\alpha = 0$. If $\alpha = 0$ the assumed form (2.1) for the specific heat is wrong. The form

$$C_H/k \sim -A \log(1 - K/K_c) + B \qquad (K \to K_c) \qquad (4.5)$$

would be more appropriate. If this assumption is true the first temperature derivative of the specific heat would have a simple pole and Padé approximants to $(d/dK)C_H$ should converge rapidly in the neighbourhood of the critical point. In Table 4.2 the physical root of the Padé approximants to $(d/dK)C_H$ are listed. The approximants seem to be converging rapidly towards the assumed critical point $K_c = 0.2210$. The "best" estimate of K_c from this Table is $K_c = 0.2203$. This estimate is remarkably close to the estimate from the fluctuation series. The convergence in this Table is extraordinary, especially when compared with the convergence of the estimates of K_c in Table 4.1 which assumes a function of the form (2.1) near the critical point. Clearly, $(d/dK)C_H$ must be very close approximation to a simple pole in the critical region, and the XY model specific heat will be closely approximated by (4.5), except possibly very near the critical point.

If the form (4.5) is assumed, then estimates of the critical amplitude A can be obtained by evaluating Padé approximants to

$$(K - K_c)(d/dK)\, C_H \tag{4.6}$$

at the critical point $K_c = 0.2210$. Estimates are given in Table 4.3. A best estimate A from this Table is $A = 0.254 \pm 0.06$. Hence

Table 4.2

Estimates of K_c from Padé approximants to $(d/dK)C_H$.

Approximant [L,M]	Physical root
[4,6]	0.2199
[5,5]	0.2199
[6,4]	0.2208
[7,3]	0.2205
[3,6]	0.2201
[4,5]	0.2200
[5,4]	0.2111
[6,3]	0.2219
[3,5]	0.2198
[4,4]	0.2176
[5,3]	0.2181
[6,2]	0.2096
[2,5]	0.2191
[3,4]	0.2102
[4,3]	0.2163
[5,2]	0.2100

Table 4.3

Estimates of A from evaluating Padé approximants to $(K - K_c)(d/dK)C_H$ at $K_c = 0.2210$.

Approximant [L,M]	Value
[4,6]	0.2510
[5,5]	0.2365
[6,4]	0.2548
[7,3]	0.2547
[3,6]	0.2583
[4,5]	0.2586
[5,4]	0.2533
[6,3]	0.2546
[3,5]	0.2542
[4,4]	0.2516
[5,3]	0.2596
[6,2]	0.2554
[2,5]	0.2498
[3,4]	0.2501
[4,3]	0.2463
[5,2]	0.2508

$$C_H/k \sim -0.254 \log(1 - K/K_c) - 0.254 \quad (K \to K_c) \; . \qquad (4.7)$$

A possible simple "mimic" function for the XY model specific heat is

$$C_H/k \sim -0.254[\log(1 - K/K_c) + K/K_c] + \phi(K) \qquad (4.8)$$

where $\phi(K)$ is the correction polynomial.

The proposed functional form (4.7) for the limiting behavior of the XY model specific heat is tentative. More terms for the f.c.c. specific heat series will be needed to verify this assumed behavior.

CHAPTER 5

COMPARISON WITH EXPERIMENT

5.1 The Ising Model

Recently (Huiskamp 1972) good agreement has been found between experimental measurements of the specific heat on the Ising-like material Rb_3CoCl_5 and numerical predictions for the simple cubic Ising model specific heat. The experimental results were found to fit rather well to the curve

$$C/k \sim A[(1 - T_n/T)^{-1/8} - 1 - T_n/8T] \qquad (5.1)$$

where $T_n = 1.14$ K is the antiferromagnetic Neél point. This is the same functional form as suggested by Hunter (1968) for the three dimensional specific heat of the Ising model. The specific heat of Cs_3CoCl_5 also appeared to fit the functional form (5.1) very well (Huiskamp 1972).

These are the only Ising-like materials which at present seem to give an estimate of $\alpha = 1/8$. Most of the other Ising-like materials seem to be fitted better to a curve with $\alpha \approx 0.31$ (Cooke et al 1972). There seems to be some experimental evidence for $\alpha = 1/8$ but at present the evidence is not overwhelmingly in favor of this value. Hopefully higher resolution and better estimates of the critical temperatures in experiments will soon resolve this problem.

5.2 The XY Model

He^4 near the superfluid transition temperature T_λ is expected to behave like an XY model system (Matsubara and Matsuda 1956). This substance has also been examined in more detail experimentally than any other "XY like" material. In fluid systems like He^4, the heat capacity at constant pressure is the analogue of the specific heat at constant field in magnetic systems.

Ahlers (1969) has found that the experimental curve for C_p does not disagree with $\alpha = 0$ and his three alternative interpretations of the data all had $\alpha \leq 0.001$. More recent experimental results on He^4 by Ahlers (1972) (private communication) fit very well (assuming $\alpha = \alpha'$) to

$$C_p = \frac{A}{\alpha}[1 + b\tau^x][\tau^{-\alpha} - 1] + B$$

for (5.2)

$$0.03 \geq \alpha = \alpha' \geq 0.02$$

and

$$0.5 < x < 0.9 \; .$$

This is a very good agreement with the assumed theoretical behavior of the XY model. The results of Chapter 4 are not precise enough to rule out the

possibility that α is a small power and experiments do not rule out that $\alpha = 0$. Experimental and theoretical calculations seem to generally agree, but work needs to be done in both fields to resolve whether α is a small power or is equal to zero.

PART II

A NEW TECHNIQUE IN THE ANALYSIS OF EXACT SERIES EXPANSIONS IN LATTICE STATISTICS

CHAPTER 6

LOW TEMPERATURES SERIES EXPANSIONS FOR THE ISING MODEL OF A FERROMAGNET

In this chapter a new technique in the analysis of exact series expansion in lattice statistics will be presented. This technique is applied to the exact low temperature-high field expansion of the magnetization of the Ising model.

The low temperature series expansion is an expansion about the ordered state. For temperatures slightly above absolute zero the ordered state will be perturbed by thermal excitations. The probability of any perturbation from the ordered state is given by the appropriate Boltzmann factor. In general, overturning of almost any spin causes an increase in energy and the most important perturbation at the lowest temperature will correspond to a relatively few overturned spins. Then one can group the perturbations conveniently according to the number of overturned spins, the energy of any particular perturbation depending on the relative positions of these spins. More precisely, the increase in energy of a perturbation is given by

$$\Delta E = 2J(qs - 2r) + 2mHs \tag{6.1}$$

where q is the coordination number, H the applied field, s the number of overturned spins and r the number of nearest neighbour pairs in the overturned configuration.

Denoting $\exp(-2J/k_BT)$ by z and $\exp(-2mH/k_BT)$ by μ, the Boltzmann factor corresponding to (6.1) will be $z^{qs-2r}\ \mu^s$. At sufficiently low temperatures both z and μ will be small and the partition function and free energy can be expanded as a double series in powers of z and μ.

Denoting N as the number of sites on a lattice, the number of perturbations for the ordered state corresponding to a given Boltzmann factor will be a polynomial in N. The configurational free energy per spin is proportional to the logarithm of the configurational partition function and it can be shown (Domb 1960) that this corresponds to taking the coefficient of the first power of N in the partition function. Hence, letting the linear part of the total number of ways of choosing s spins with r bonds by [s;r], then the logarithm of the partition function per site is given by

$$\log \Lambda = \sum_{\text{all } s,r} [s;r]\ z^{qs-2r}\ \mu^s \quad . \tag{6.2}$$

It is customary to group the expansion (6.2) as a series either in powers of μ, written as

$$\log \Lambda = \sum_s L_s(z)\ \mu^s \tag{6.3}$$

where $L_s(z)$ are called the low temperature polynomials

and are finite polynomials in z, or in powers of z, written as

$$\log \Lambda = \sum_n \psi_n(\mu)\, z^n \tag{6.4}$$

where the $\psi_n(\mu)$ are finite polynomials in μ. Using this notation the free energy per spin will then be given by

$$F = -\frac{1}{2}\, qJ - mH - kT \log \Lambda \quad . \tag{6.5}$$

When using the method outlined above, one usually groups the perturbations according to the topology of their nearest neighbor linkages. To illustrate the use of this method, consider the perturbations of four spins and three nearest neighbor bonds on the f.c.c. lattice. [4;3] consists of the following perturbations together with the number of ways of putting each perturbation on the lattice

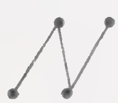

282 N

44 N

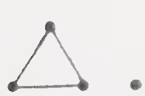

$(8\ N^2 - 200\ N)$

Hence, the coefficient of $z^{42}\ \mu^4$ is 126. Many very sophisticated techniques have been developed for counting such low-temperature configurations (Domb 1960, Sykes et al 1965, 1973).

The tests in this chapter were made possible by recently extended data on the low temperature expansion of the free energy on the two and three dimensional Ising models (Sykes et al 1965, 1973). The low temperature series expansion on the two dimensional lattices are now complete to the $L_{21}(z)$ polynomial in the (6.3) grouping and the $\psi_{16}(\mu)$ polynomial in the (6.4) grouping for the honeycomb, $L_{15}(z)$ and $\psi_{22}(\mu)$ for the square, and $L_{10}(z)$ and $\psi_{32}(\mu)$ for the triangular. The three dimensional diamond lattice is complete to $L_{17}(z)$ and $\psi_{30}(\mu)$. The tests were also used on the hydrogen peroxide lattice data, developed by Dr. D.D. Betts and his group at the University of Alberta. The hydrogen peroxide lattice is complete to $L_{21}(z)$ and $\psi_{16}(\mu)$.

CHAPTER 7

SCALING AND THERMODYNAMIC RELATIONS FOR INDICES

7.1 Thermodynamic Inequalities

The only rigorous relations thus far proposed among the critical-point exponents are a set of inequalities. Using the stability-convexity relations

$$C_M(H,T) = -T\left(\frac{\partial^2 F}{\partial T^2}\right)_M \geq 0 \tag{7.1}$$

and

$$\frac{1}{\chi_T(H,T)} = \left(\frac{\partial^2 F}{\partial M^2}\right)_T \geq 0 \tag{7.2}$$

with standard thermodynamic manipulations Rushbrooke (1963) rigorously proved for any system

$$\alpha' + 2\beta + \gamma' \geq 2 . \tag{7.3}$$

(We use the widely accepted notation for critical exponents; see Fisher (1967), for example).

A further important inequality

$$\alpha' + \beta(1 + \delta) \geq 2 \tag{7.4}$$

was rigorously established by Griffiths (1965), by the use of very general convexity properties of the free energy.

For the Ising model, Buckingham and Gunton (1968) proved the inequalities

$$2 - \eta \leq d(\delta - 1)/(\delta + 1) \tag{7.5}$$

and

$$2 - \eta \leq d\gamma'/(2\beta + \gamma') \leq d\gamma'/(2 - \alpha') \qquad (7.6)$$

where d is the dimensionality and more recently Fisher (1969) showed

$$\gamma \leq (2 - \eta)\nu \quad . \qquad (7.7)$$

Very recently Griffiths (1972) proved for the Ising model that the magnetization on any path, which in the critical region is of the form,

$$\tau \propto H^p \quad , \qquad (7.8)$$

must have a critical exponent with a value less than or equal to β. The proof of this inequality follows directly from the convexity of the Gibbs free energy.

If $M_p(H,T)$ denotes the magnetization on the path defined by (7.8), β_p the critical exponent of $M_p(H,T)$ near the critical point, $M(0_+, T)$ the spontaneous magnetization, and τ the reduced temperature $(T_c-T)/T_c$, then

$$M_p(H,T) \propto \tau^{\beta_p} \qquad (7.9)$$

and

$$M(0_+, T) \propto \tau^{\beta} \quad . \qquad (7.10)$$

Since the Gibbs function is convex

$$\left(\frac{\partial M}{\partial H}\right)_T \geq 0 \quad . \tag{7.11}$$

This implies the projection of the slope in the H direction, on the M(H,T) surface is always positive. Therefore along an isotherm in the positive H direction the magnetization will remain unchanged or increase in value. This is shown geometrically in Figure 7.1. The solid curved line represents the spontaneous magnetization, the broken curved line is any path of the form (7.8) and T_c is the critical point.

Therefore

$$M_p(H,T) \geq M(0_+, T) \quad . \tag{7.12}$$

Equations (7.9), (7.10), and (7.12) imply

$$\tau^{\beta_p} \geq \tau^{\beta} \quad . \tag{7.13}$$

Hence, as τ approaches zero

$$\beta \geq \beta_p \qquad \text{for all } p \ . \tag{7.14}$$

In a private communication Griffiths has stated that he has shown from the Kelly-Sherman inequalities (Kelly and Sherman 1968, Griffiths 1967) that

$$\frac{1}{\delta} \geq \beta_p \qquad \text{for all } p > 1 \quad . \tag{7.15}$$

FIGURE 7.1

THE ZERO FIELD PATH AND A TYPICAL PATH

OF THE FORM $\tau \propto h^p$ ON THE M(H,T) SURFACE

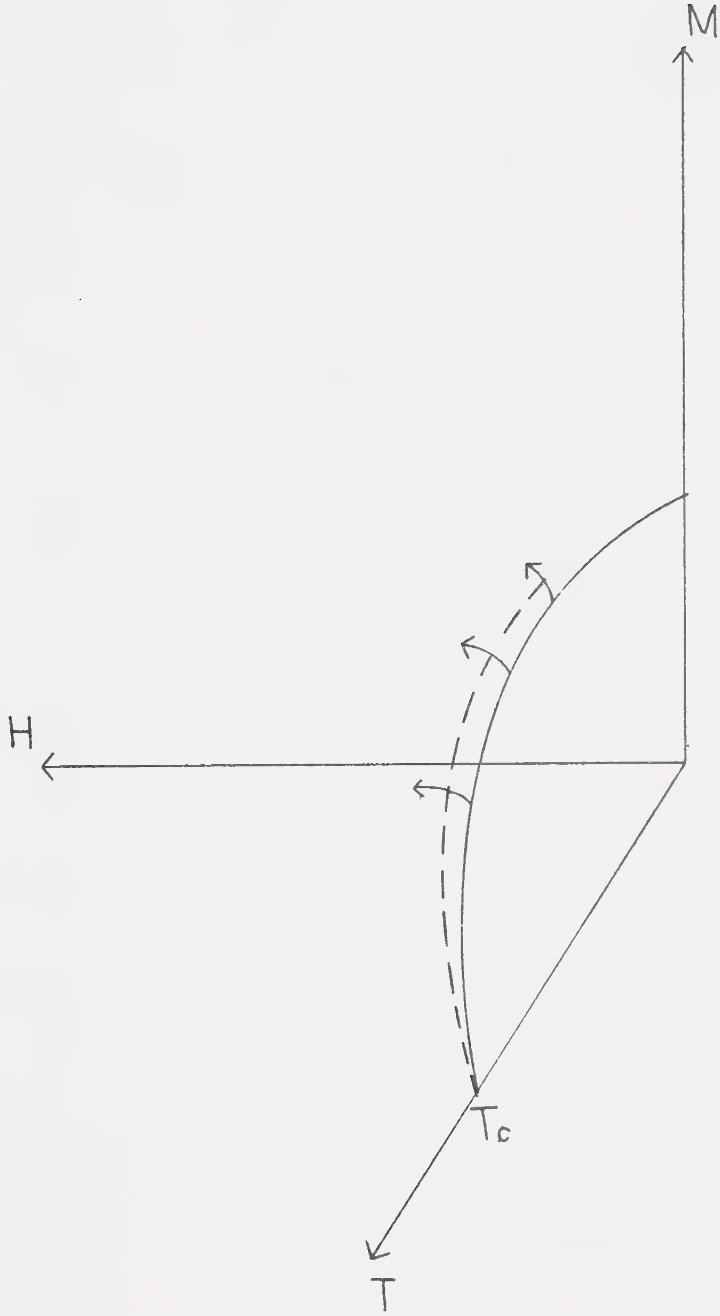
M
H
T_c
T

By making some quite plausible but more special and less fundamental assumptions, a variety of further inequalities can be derived (Stanley 1971, Stephenson 1971). The above inequalities are of particular utility when used with results derived from series analysis and experiments.

7.2 Scaling Theory

It has been conjectured by Essam and Fisher (1963) that (7.3) can be replaced by the equality but so far no rigorous proof exists although the conjecture is consistent with experimental and model calculations and the non-rigorous scaling-law theory of exponents which predicts that the inequalities (7.3-7.7, 7.14, 7.15) are equalities.

The scaling hypothesis was suggested by Widom (1965 a,b), Domb and Hunter (1965), Kadanoff et al (1967) and Patashinskii and Pokrovskii (1966). The basic postulate of the static scaling hypothesis asserts that the Gibbs potential $G(\tau,H)$ is a generalized homogeneous function. A function $f(X,Y)$ is by definition homogeneous if for all values of the parameter λ,

$$f(\lambda^a X, \lambda^b Y) = \lambda f(X,Y) \quad . \tag{7.16}$$

Thus from the general definition of (7.16), the static scaling hypothesis states

$$G(\lambda^{a}H,\ \lambda^{b}\tau) = \lambda G(H,\tau) \quad . \tag{7.17}$$

Differentiating both sides of (7.17) with respect to the field derivative H,

$$M(H,\tau) = \lambda^{a-1}\ M(\lambda^{a}H,\ \lambda^{b}\tau) \quad . \tag{7.18}$$

Letting $\lambda = (1/\tau)^{1/b}$ and evaluating (7.18) along the axis $H = 0$, β is found to be

$$\beta = \frac{1 - a}{b} \quad . \tag{7.19}$$

Setting $\lambda = H^{-1/a}$ in (7.18) and evaluating the equation along the critical isotherm it is found that

$$\delta = \frac{a}{1 - a} \quad . \tag{7.20}$$

Equations (7.19) and (7.21) can be solved simultaneously for the scaling parameters a and b, and then substituted into (7.18) to give the magnetic equation of state,

$$M(H,\tau) = \lambda^{-1}\ M(\lambda^{\delta}H,\ \lambda^{1/\beta}\tau) \ , \tag{7.21}$$

where (new λ) = (old λ)$^{1/1+\delta}$.

Putting $\lambda = \tau^{-\beta}$ or $\lambda = H^{-1/\delta}$, two alternate forms for (7.21) are possible,

$$M(H,\tau) = \tau^{\beta}\ M_1(H/\tau^{\Delta}) \tag{7.22}$$

and

$$M(H,\tau) = H^{1/\delta}\ M_2(\tau/H^{1/\Delta}) \tag{7.23}$$

where M_1 and M_2 are analytic in the vicinity of the origin and $\Delta = \beta\delta$.

One can obtain additional exponents by taking the second derivative of (7.17) with respect to the field to get the isothermal susceptibility and by differentiating twice with respect to temperature to obtain the specific heat at constant field. This yields

$$\gamma' = \gamma = \beta(\delta - 1) \quad , \qquad (7.24)$$

$$\alpha' + \beta(\delta + 1) = 2 \quad , \qquad (7.25)$$

$$\alpha' + 2\beta + \gamma' = 2 \quad , \qquad (7.26)$$

and

$$\alpha = \alpha' \quad . \qquad (7.27)$$

It should be clear how to obtain all the critical exponents in terms of the scaling parameters a and b , and how these two parameters are eliminated to obtain a whole host of equalities among the exponents. It is also noted that the inequalities of section 7.1 all become equalities in scaling theory.

7.3 Tests of Scaling Theory

For experimental magnetic systems or, with appropriate identification of variables, for fluids the scaling hypothesis can be tested by fitting a scaled equation

of state to the data (M. Vicentini-Missoni et al, 1969 and references therein). More sensitive tests can be achieved with theoretical models, in particular the Ising model. The critical exponents derived from series analysis techniques can be used to test the various equalities (equations 7.24-7.27 etc...) predicted by scaling theory (Kadanoff et al 1967). The scaled equation of state can be constructed by the use of analytic continuation methods on series expansions and then the theoretical expectations resulting from the form of the equation of state are checked against series expansion results (Gaunt and Domb 1970). The critical behavior of the magnetization and its temperature derivatives can be examined on the critical isotherm and the estimates of the critical exponents compared with scaling predictions (Betts and Filipow 1972). The series expansions of the higher derivatives of the free energy with respect to the magnetic field can be studied above and below the critical point to verify scaling predictions (Essam and Hunter 1968). All these tests have given good agreement with scaling and none contradicts scaling. Relations among critical amplitudes are also obtainable from scaling theory (Watson 1969, Betts, Guttmann and Joyce 1971) and they too seem to be satisfied by models such as the Ising model (Gaunt and Domb 1970, Betts and Filipow 1972). The next chapter will put forward a new test of the predictions of scaling theory.

CHAPTER 8

A NEW TEST OF SCALING IN THE CRITICAL REGION

Equations (7.22) and (7.23) yield predictions of the critical exponents of the magnetization and its derivatives along the τ and H axes and these are the exponents usually examined and tested. The above scaling theory equations also tell us something about the magnetization along any path which in the critical region is of the form (7.8).

Along this path (7.22) and (7.23) become

$$M(H,\tau) = \tau^{\beta} M_1(\tau^{(1-p\Delta)/p}) \tag{8.1}$$

and

$$M(H,\tau) = H^{1/\delta}\, M_2(H^{(p\Delta-1)/\Delta}) \quad . \tag{8.2}$$

From equations (8.1) and (8.2) it can be seen that the quadrant $H \geq 0$, $\tau \geq 0$ is divided into two regions by the curve $\tau = H^{1/\beta\delta}$. For curves with $p < 1/\beta\delta$ all exponents have their τ axis value as given by (7.22) while for $p \geq 1/\beta\delta$ all exponents have their H axis value determined from (7.23).

These predictions from scaling theory are much stronger than the thermodynamic inequalities (7.14) and (7.15) by Griffiths. It is noted that thermodynamic inequalities have once again been shown to be equalities in scaling theory. The predictions can be tested in the case of the two and three dimensional Ising models where extensive data are available in the low temperature-high

field expansion of the free energy. From Chapter 6 one sees that the free energy is expressed as a power series in the variables $\mu = \exp(-2mH/k_BT)$ and $z = \exp(-2J/k_BT)$. It is convenient to replace z by $s = z/z_c$ in the expansions. Figure 8.1 depicts schematically the (s,μ) plane showing the critical point, (1,1), the path $\mu = 1$ and $s = 1$ along which the behavior of thermodynamic functions is usually examined and the critical curve $s = 1-(1-\mu)^{1/\beta\delta}$ (broken line) dividing the area of interest into two regions and the paths

$$s = 1 - (1 - \mu)^p \tag{8.3}$$

along which the critical behavior of the magnetization was investigated in this thesis.

From (6.3) and (6.5) and the definition of the magnetization, the magnetization in the variables μ and z is given by

$$M(\mu,z) = m[1-2\mu(\partial L/\partial\mu)_z] \ . \tag{8.4}$$

Using this definition a computer program was written to derive series for various paths defined by (8.3) from the low temperature polynomials of the honeycomb, square, triangular, hydrogen peroxide, and diamond lattices. In the cases of the square, triangular and diamond lattices s was defined as $s = u/u_c = (z/z_c)^2$.

FIGURE 8.1

PATHS ON WHICH THE MAGNETIZATION WAS STUDIED

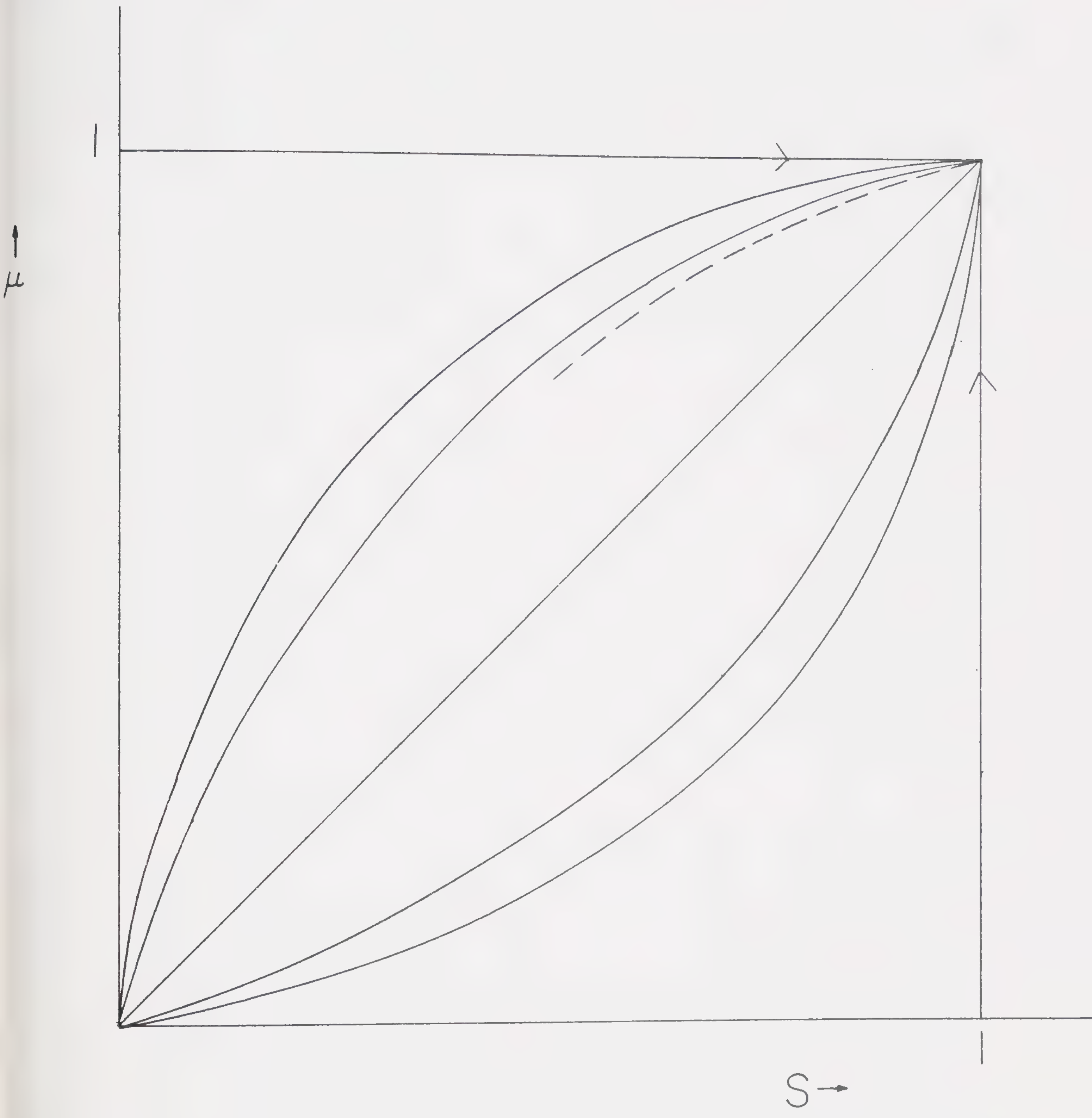
1
μ
1
S

For the derivation of these series (8.3) must be expanded by the binomial expansion. If p is non-integral, the truncated series expansion will be a very poor representation of (8.3) near the critical point. For this reason only integral values of p can be used in (8.3). This will give series for the diagonal path $s = \mu$ and above. Below the diagonal path (8.3) must be inverted, i.e.

$$\mu = 1 - (1 - s)^{1/p} \quad . \qquad (8.5)$$

This can be expanded for integral values of 1/p and series below the diagonal path can be studied. A second consideration is that for a curved path, the closer the path is to the diagonal path the more of the expansion data is used. For this reason only small integral values of p and 1/p are studied.

The paths along which the magnetization was studied for the five lattices are shown schematically in figure 8.1 and these are the paths for p = 3, 2, 1, 1/2, and 1/3, plus the critical isotherm and zero field paths. For the two dimensional Ising model $\beta\delta = 1.875$ and for the three dimensional Ising model $\beta\delta \approx 1.56$. Thus, scaling theory predicts the magnetization on the critical isotherm and on the critical paths for p = 1, 2, and 3 must have critical indices equal to $1/\delta$ for both the two and three dimensional Ising models. The zero field

magnetization and the magnetization on the critical paths for $p = 1/2$ and $1/3$ must have critical indices equal to β for both models.

The critical points for the two dimensional lattices are known exactly, so all the series derived for these lattices are exact. For the three dimensional lattices the critical points are not known exactly. The locations of the critical points have been determined by the author from a reanalysis of the high temperature susceptibility series of both lattices (Essam and Sykes 1963, Leu, Betts and Elliott 1969). The critical points used were $z_c = 0.317393$ for the hydrogen peroxide lattice and $u_c = z_c^2 = 0.227832$ for the diamond lattice.

The series derived by this method are very long on some of the paths. This length is deceptive since there is actually less configurational information in these long series than there is in the series for the spontaneous magnetization or the magnetization on the critical isotherm, which are much shorter. For instance, on the honeycomb lattice the spontaneous magnetization is complete to z^{16}, the magnetization on the critical isotherm is complete to μ^{21}, and the magnetization on the path for $p = 2$ is complete to s^{39}. The magnetization series for all the paths on the five lattices are given in the Appendix.

CHAPTER 9

ANALYSIS OF THE SERIES

9.1 Arbitrary Curved Path Series

Most of the magnetization series on the various paths have coefficients which vary erratically in sign and magnitude, and therefore the ratio method (Domb and Sykes 1957) and variations of it cannot be used. The critical isotherm series, the zero field magnetization series, and some of the diagonal series have smoother ratios but unfortunately in no case have the ratios become linear in $1/n$. They all exhibit an irregular oscillation probably due to the influence of competing non-physical singularities of the order of unit distance from the origin in the complex plane of μ or s. Figure 9.1 is a plot of the smoothest set of ratios. In this figure, the ratios of the coefficients of the magnetization of the triangular lattice on the critical isotherm are plotted against $1/n$. From this plot it is estimated $1/\delta = 0.064 \pm 0.02$. In Table 9.1 successive linear approximations to the exponent, given an exact value of the critical point $\mu_c = 1$, are tabulated, using equation (2.4). This series is fluctuating too much to give a precise estimate of $1/\delta$. The ratios of the coefficients for this particular series are far more regular than the ratios of the other 32 series analyzed. The estimates from ratio plots, though imprecise, have been done to give confidence limits and to check other results. The

FIGURE 9.1

RATIOS μ_n VS. $1/n$ FOR THE MAGNETIZATION OF THE TRIANGULAR LATTICE ON THE CRITICAL ISOTHERM.

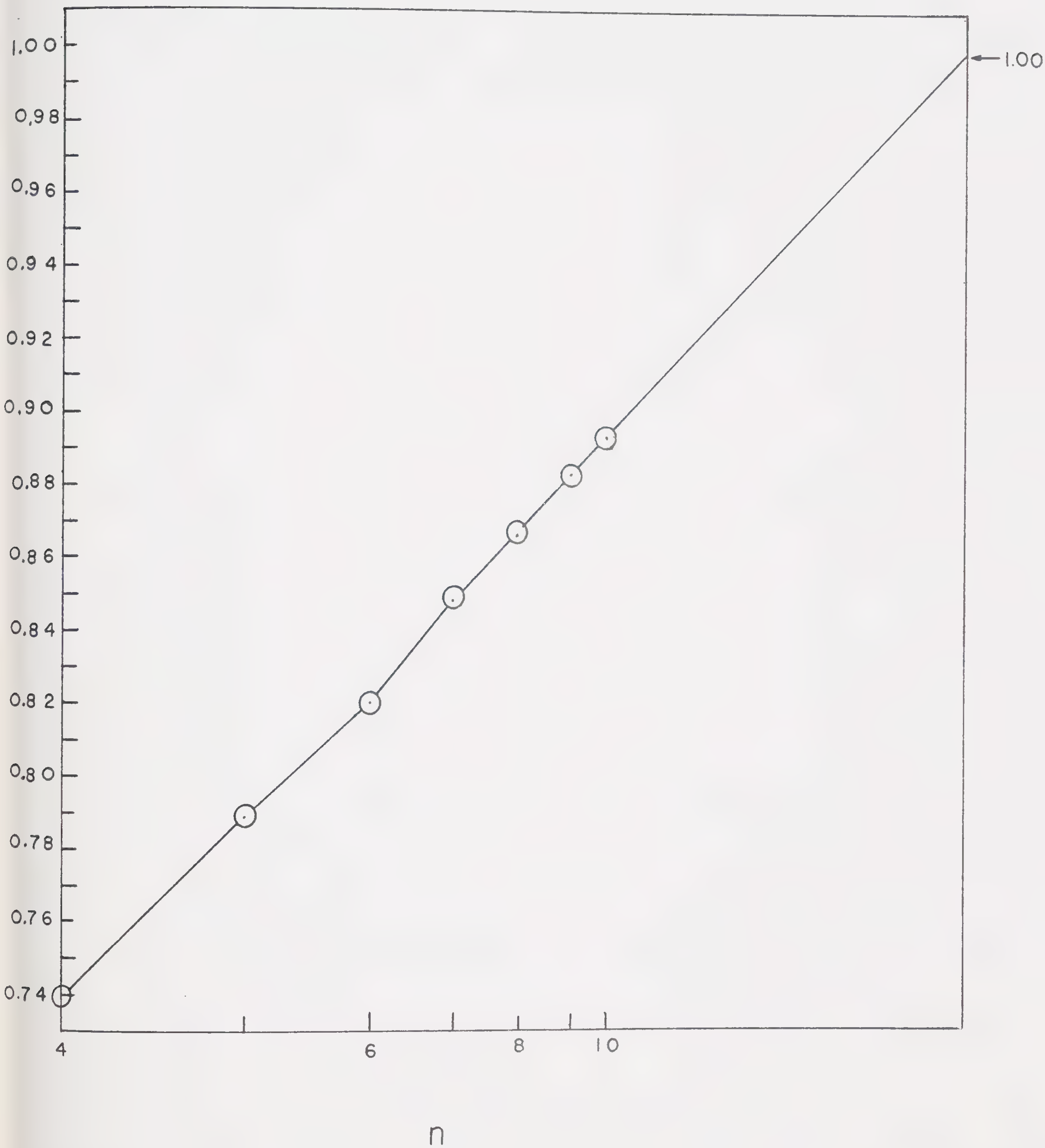

1.00
0.98
0.96
0.94
0.92
0.90
0.88
0.86
0.84
0.82
0.80
0.78
0.76
0.74
1.00
4
6
8
10
n

Table 9.1

Sequence of approximations to the exponent given the critical point $\mu_c = 1$ for the triangular magnetization on the critical isotherm, using the equation $\gamma(n) = n(1 - \mu_n) - 1$.

n	$\gamma(n)$
1	0.07407
2	0.18519
3	0.05051
4	0.04088
5	0.05510
6	0.07728
7	0.05631
8	0.05896
9	0.06892
10	0.06117

ratio method agreed with other methods on all series except the diagonal series. The reasons for this discrepancy will be discussed later.

Four different techniques other than the ratio method were used to analyze the series to obtain estimates of the critical exponents and three of the tests gave very precise and consistent results and the fourth method gave better confidence limits, on some of the series, than the ratio method. The three tests which gave very consistent results were all variations of Padé approximant techniques.

The first method consists of the determining of the poles and residues of the Padé approximants (Baker 1961) to the logarithmic derivative of the magnetization on the various paths. The poles give estimates of the critical point and the residues give estimates of the critical exponent. In Table 9.2, the location of the pole and the value of the residue for a few of the Padé approximants are tabulated for the path $s = 1 - (1-\mu)^{\frac{1}{2}}$ on the square and hydrogen peroxide lattices. It was noted that the location of the pole and the value of the residue seem to follow a smooth relationship for all Padé approximants. When plotted the two estimates form a very smooth curve for both series. The intersection of this curve with the line s = 1 is a "best" estimate of the exponent. The resulting curves for the

Table 9.2

Padé approximants to (d/ds)log M(s) on the path $s = z/z_c = 1 - (1 - \mu)^{\frac{1}{2}}$ on the square and the hydrogen peroxide lattices.

Hydrogen Peroxide			Square		
Approximant [L,M]	Singularity	Residue	Approximant [L,M]	Singularity	Residue
[16,20]	0.9991	0.3131	[11,13]	0.99948	0.1253
[17,19]	0.9987	0.3109	[12,12]	1.00064	0.1279
[18,18]	0.9994	0.3149	[13,11]	1.00076	0.1281
[19,17]	0.9988	0.3114	[14,10]	1.00010	0.1269
[20,16]	0.9976	0.3051	[15, 9]	1.00021	0.1271
[15,20]	0.9989	0.3121	[9,14]	1.00081	0.1281
[16,19]	0.9985	0.3098	[11,12]	1.00157	0.1292
[17,18]	0.9978	0.3065	[12,11]	1.00084	0.1282
[18,17]	1.0121	0.4348	[13,10]	1.00088	0.1283
[19,16]	0.9975	0.3048	[14, 9]	0.99983	0.1264
[15,19]	0.9982	0.3087	[10,12]	1.00246	0.1300
[16,18]	0.9978	0.3064	[11,11]	1.00345	0.1306
[17,17]	0.9978	0.3064	[12,10]	1.00071	0.1280
[18,16]	0.9970	0.3025	[13, 9]	1.00168	0.1295
[19,15]	0.9976	0.3052	[14, 8]	0.99814	0.1235
[14,19]	0.9987	0.3109	[18,13]	1.00166	0.1292
[15,18]	0.9984	0.3096	[9,12]	1.00213	0.1298
[16,17]	0.9978	0.3065	[10,11]	1.00194	
[17,16]	1.0043	0.3501	[11,10]	1.00149	
[18,15]	0.9975	0.3047	[12, 9]	0.99917	

path $s = 1 - (1 - \mu)^{\frac{1}{2}}$ on the triangular and hydrogen peroxide were very similar to the curve shown in Figure 9.4 which is the same plot for the honeycomb diagonal series. The intersection points are found to be 0.1265 on the square lattice and 0.319 on the hydrogen peroxide lattice. The plot of location of the critical point versus the residue forms a very regular and smooth curve for all the other series and appears to give a very precise estimate of the exponents.

The second method consists of determining the Padé approximants to the series for

$$(1 - \mu)(d/d\mu) \log M(\mu)$$

or

$$(1 - s)(d/ds) \log M(s)$$

or

$$(z - z_c)(d/dz) \log M(z) \tag{9.1}$$

and evaluating the Padé approximants at the critical points ($\mu = 1$, $s = 1$, or $z = z_c$) to give estimates of the critical exponents. Table 9.3 represents typical Padé evaluation tables for the two and three dimensional lattices studied. From this Table a "best" estimate of the critical exponent for the triangular and diamond on the path $s = 1 - (1 - \mu)^{\frac{1}{3}}$ is 0.12495 and 0.3115 respectively. The scatter of the numerical values of the

evaluations of the Padé approximants to (9.1) in Table 9.3 are typical of the scatter in the Padé evaluations of all the series tested. It was also noted that the higher degree Padé evaluations appear to be converging towards the scaling predictions. In all cases the results from this method agree very well with method 1.

The third method involves making Padé approximants to various powers of the magnetization on a given path and then plotting the location of the pole versus the power for a few of the Padé approximants. The intersection of these curves with the line corresponding to the critical point gives a "best" estimate of the exponent. Figure 9.2 is such a plot for the series on the path $s = 1 - (1 - \mu)^2$ for the square lattice. From this plot a "best" estimate of the exponent is 0.0654. This method gives results very consistent with methods 1 and 2.

These methods were the only methods which gave any consistent results for many of the series. A fourth method which worked successfully on the series for the zero field magnetization and the magnetization on both the critical isotherm and the diagonal paths was the numerical evaluation of the series to the function (9.1) at the critical point using successively higher coefficients of the series. This series should form a sequence of estimates converging on the critical exponent. If the sequence is regular the last value can be taken as either

FIGURE 9.2

LOCATION OF THE POLE L VS. THE POWER P FOR A FEW PADÉ APPROXIMANTS TO $[M_2(\mu)]^P$ FOR THE SQUARE LATTICE ON THE PATH $s = 1 - (1 - \mu)^2$.

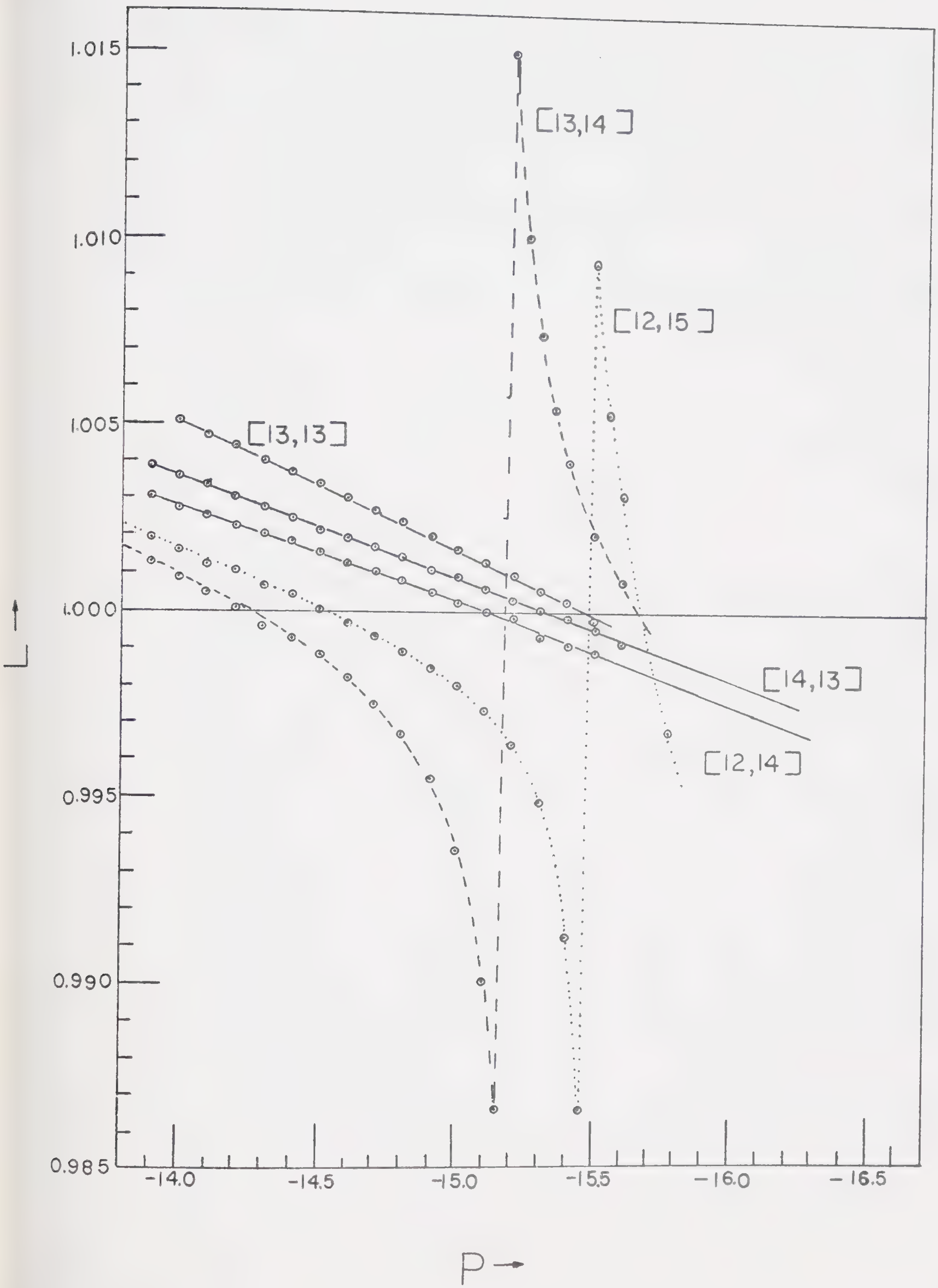

1.015
1.010
1.005
1.000
0.995
0.990
0.985
-14.0
-14.5
-15.0
-15.5
-16.0
-16.5
[13,14]
[12,15]
[13,13]
[14,13]
[12,14]
L
P

Table 9.3

Evaluation of Pade approximants to $(1-s)(d/ds)\log M$ at the critical point $s = 1$ for the path $s = z/z_c = 1-(1-\mu)^{1/3}$ on the triangular and diamond lattices.

Triangular		Diamond	
Approximant	Value	Approximant	Value
[12,14]	0.12491	[15,17]	0.31201
[13,13]	0.124998	[16,16]	0.31258
[14,12]	0.124996	[17,15]	0.31200
[15,11]	0.12478	[18,14]	0.30910
[11,14]	0.12503	[14,17]	0.31142
[12,13]	0.12481	[15,16]	0.31183
[13,12]	0.12502	[16,15]	0.31177
[14,11]	0.12492	[17,14]	0.30659
[11,13]	0.12492	[14,16]	0.31240
[12,12]	0.12502	[15,15]	0.31143
[13,11]	0.12502	[16,14]	0.31627
[14,10]	0.12482	[17,13]	0.30975
[10,13]	0.12497	[13,16]	0.31779
[11,12]	0.12520	[14,15]	0.31059
[12,11]	0.12502	[15,14]	0.31012
[13,10]	0.11994	[16,13]	0.29340

an upper or lower bound. These sequences for the magnetization on the critical isotherm for the honeycomb and hydrogen peroxide lattices are shown in Table 9.4. From these sequences it can be estimated that $1/\delta > 0.0659$ for the honeycomb lattice and $1/\delta > 0.1840$ for the hydrogen peroxide lattice. When the inaccuracies in the critical point are considered it is found that $1/\delta > 0.180$ for hydrogen peroxide. Thus we get lower bounds for $1/\delta$ in both two and three dimensions and we can use these values as confidence limits. All the confidence limits quoted in this section are a result of this method or the ratio method.

Tables 9.5 and 9.6 are a summary of the results of these various methods. The number of significant figures quoted represents the apparent precision of the various consistent results and has nothing to do with the actual accuracy of the results. Since many of these seemingly very precise results differ from lattice to lattice the various estimates of the exponents have not converged as much as the methods seem to indicate. For this reason no confidence limits are quoted where the ratio method and method 4 gave no results.

The two dimensional results agree remarkably with scaling on all paths but the diagonal. In all cases other than the diagonal the estimates are within a few

Table 9.4

Value of $(\mu - 1)(d/d\mu) \log M$ at the critical point $\mu = 1$ using each successive coefficient of the critical isotherm magnetization series for the honeycomb and hydrogen peroxide lattices.

Degree of Polynomial evaluated	Numerical value of polynomial	
	Honeycomb	Hydrogen Peroxide
1	0.05742	0.10951
2	0.06262	0.13546
3	0.06199	0.15098
4	0.05884	0.16053
5	0.06318	0.16643
6	0.06518	0.16997
7	0.06503	0.17191
8	0.06348	0.17274
9	0.06486	0.17386
10	0.06554	0.17522
11	0.06522	0.17659
12	0.06507	0.17783
13	0.06556	0.17895
14	0.06561	0.17993
15	0.06561	0.18077
16	0.06570	0.18151
17	0.06577	0.18217
18	0.06584	0.18282
19	0.06590	0.18341
20	0.06590	0.18396

Table 9.5

Two dimensional Ising model magnetization critical exponent on various paths

Path analyzed	Expected exponent from scaling	Results from analysis of honeycomb lattice series	Results from analysis of square lattice series	Results from analysis of triangular lattice series
$\mu = 1$	1/8 (exact)	0.1250	0.1250	0.1250
$z/z_c = 1-(1-\mu)^{1/3}$	1/8	0.1237	0.1239	0.12495
$z/z_c = 1-(1-\mu)^{1/2}$	1/8	0.1266	0.1265	0.1258
$z/z_c = \mu$	1/15	$0.0765^{+0.004}_{-\underline{\quad}}$	$0.0770^{+0.003}_{-\underline{\quad}}$	$0.082^{+0.005}_{-\underline{\quad}}$
$z/z_c = 1-(1-\mu)^2$	1/15	0.0658	0.0653	0.0640
$z/z_c = 1-(1-\mu)^3$	1/15	0.0662	0.06653	0.0684
$z = z_c$	1/15	$0.06620^{+0.03}_{-0.0005}$	$0.06636^{+0.03}_{-0.0002}$	$0.06653^{+0.02}_{-0.0002}$

Table 9.6

Three dimensional Ising model magnetization critical exponent on various paths

Path analyzed	Expected exponent from scaling	Results from analysis of hydrogen peroxide lattice	Results from analysis of diamond lattice
$\mu = 1$	5/16 = .3125	$0.308 {+0.04 \atop -0.01}$	$0.311 {+0.04 \atop -0.01}$
$z/z_c = 1-(1-\mu)^{1/3}$	5/16	0.309	0.312
$z/z_c = 1-(1-\mu)^{1/2}$	5/16	0.319	0.324
$z/z_c = \mu$	1/5	0.219	0.217
$z/z_c = 1-(1-\mu)^2$	1/5	0.184	0.187
$z/z_c = 1-(1-\mu)^3$	1/5	0.182	0.186
$z = z_c$	1/5	$0.190 {+0.05 \atop -0.01}$	$0.193 {+0.04 \atop -0.01}$

percent of scaling predictions.

In three dimensions the results also agree quite well with scaling but are of an order of magnitude less precise. This is due to the imprecision in the estimate of the critical point and the critical exponents β and $1/\delta$.

9.2 Analysis of Diagonal Series

The analysis of the diagonal series for all lattices represents a very difficult problem. Figure 9.3 is a ratio plot for the honeycomb lattice. Also shown are straight lines corresponding to $\beta_1 = 1/15$, $\beta_1 = 1/8$, and $\beta_1 = 1/7$. In Table 9.7 a sequence of approximates to the exponent, given a value of the critical point $\mu = 1$, is tabulated. From the Figure 9.3 and Table 9.7 there is no evidence that with the number of terms available, the scaling value of $\beta_1=1/15$ holds and the spontaneous magnetization value of 1/8 is also implausible. The ratios do however fit rather well to the line corresponding to $\beta_1 = 1/7$.

When method 1 is used on this series the results are more consistent with scaling theory. In Table 9.8 the locations of the poles and resulting residues are tabulated for a few higher and central Padé approximants to the logarithmic derivative of the magnetization.

FIGURE 9.3

RATIOS μ_n VS. $1/n$ FOR THE HONEYCOMB MAGNETIZATION ON THE DIAGONAL PATH.

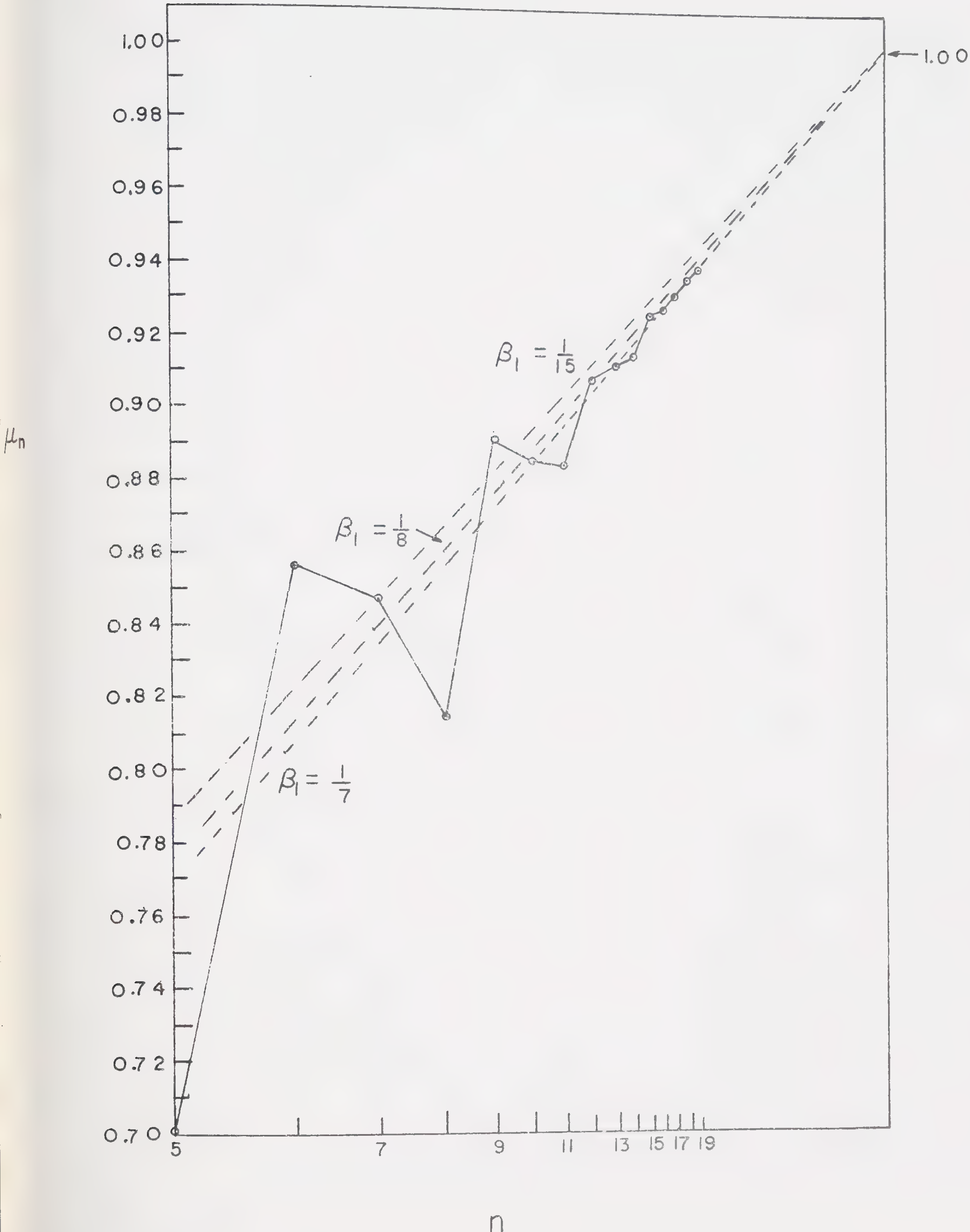

1.00
0.98
0.96
0.94
0.92
0.90
0.88
0.86
0.84
0.82
0.80
0.78
0.76
0.74
0.72
0.70
μ_n
5
7
9
11
13
15
17
19
n
1.00
$\beta_1 = \frac{1}{15}$
$\beta_1 = \frac{1}{8}$
$\beta_1 = \frac{1}{7}$

Table 9.7

Sequence of approximations to the exponent given the critical point $\mu_c = 1$ for the honeycomb magnetization on the diagonal path.

n	$\gamma(n)$
1	0.0
2	1.0000
3	-0.4115
4	0.1675
5	0.4910
6	-0.1398
7	0.0694
8	0.4754
9	-0.0185
10	0.1478
11	0.2799
12	0.0959
13	0.1462
14	0.2142
15	0.1174
16	0.1700
17	0.1612
18	0.1417
19	0.1569

Table 9.8

Padé approximants to magnetization on the diagonal path on the honeycomb lattice.

Approximant [L,M]	d/dμ log M	
	Singularity	Residue
[7,10]	1.0029	0.0835
[8, 9]	1.0014	0.0803
[9, 8]	1.0027	0.0832
[10, 7]	1.0026	0.0830
[11, 6]	1.0003	0.0774
[6,10]	1.0031	0.0839
[7, 9]	1.0033	0.0842
[8, 8]	1.0029	0.0835
[9, 7]	1.0029	0.0835
[10, 6]	1.0030	0.0837
[11, 5]	0.9969	0.0665
[6, 9]	1.0032	0.0841
[7, 8]	1.0032	0.0841
[8, 7]	1.0025	0.0828
[9, 6]	1.0043	0.0861
[5, 9]	1.0031	0.0839
[6, 8]	1.0033	0.0842
[7, 7]	1.0028	0.0833
[8, 6]	1.0028	0.0832
[9, 5]	1.0029	0.0835

The two estimates are plotted in Figure 9.4 and a very smooth curve results. The intersection of this curve with $\mu = 1$ is at the point 0.0765.

A short evaluation table of Padé approximants to the function (9.1) at the critical point $\mu = 1$ for the honeycomb diagonal series, is given in Table 9.9. A "best" estimate of the critical exponent from this table is $\beta_1 = 0.0765$.

When method 3 is used on this series the power which reproduces the known critical point the best is -13.0 which corresponds to a critical exponent of 0.0769. In Table 9.10 the evaluation of the series to function (9.1) at the critical point $\mu = 1$ using successively higher coefficient of the series is tabulated for the honeycomb diagonal series. Note the sequence is slowly convergent but very regular. This makes the upper bound of 0.07968 very probable.

When these five methods are used on the derivative to the diagonal series, the estimate for the critical exponent of the derivatives is -0.85714 for all five methods. This corresponds to a critical exponent for the magnetization on the diagonal of 0.14294 ± 0.0001 or 1/7. The results seem to fall into two contradictory groups. For the analysis of the derivative and the ratios of the magnetization on the diagonal, 1/7 is given

FIGURE 9.4

LOCATION OF THE POLE VS. THE RESIDUE AS DETERMINED FROM PADÉ APPROXIMANTS TO $(d/d\mu)\log M(\mu)$ ON THE HONEYCOMB DIAGONAL PATH.

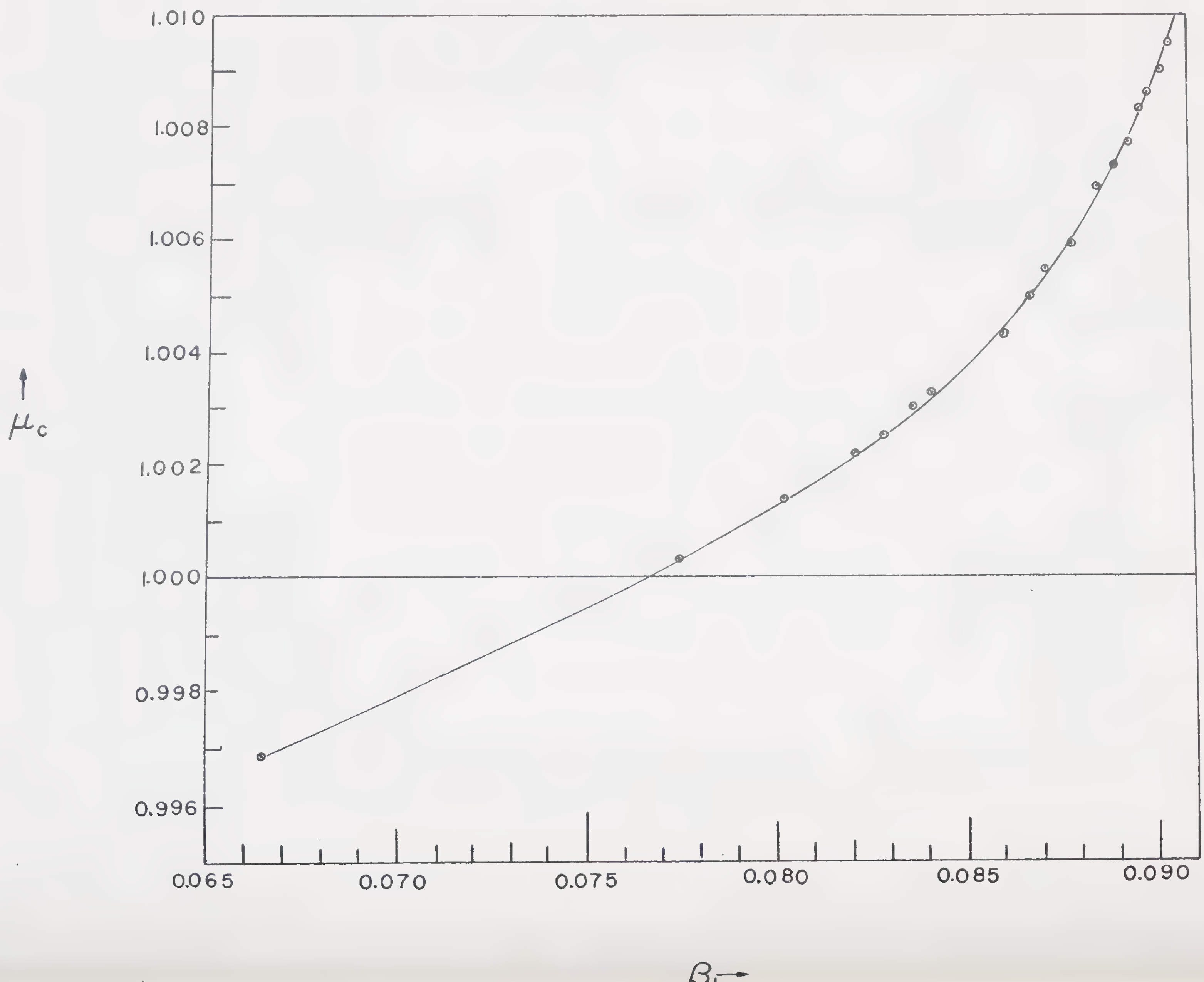

μ_c
1.010
1.008
1.006
1.004
1.002
1.000
0.998
0.996
0.065
0.070
0.075
0.080
0.085
0.090
β_1

Table 9.9

Evaluation of Pade approximants to $(1-\mu)(d/d\mu) \log M(\mu)$ at the critical point $\mu = 1$ for the diagonal series on the honeycomb lattice.

Approximant	Value
[8,10]	0.0752
[9, 9]	0.0764
[10, 8]	0.0764
[11, 7]	0.0758
[7,10]	0.0779
[8, 9]	0.0783
[9, 8]	0.0766
[10, 7]	0.0803
[7, 9]	0.0858
[8, 8]	0.0641
[9, 7]	0.0788
[10, 6]	0.0787
[6, 9]	0.0789
[7, 8]	0.0792
[8, 7]	0.0773
[9, 6]	0.0810

Table 9.10

Value of $(\mu - 1)(d/d\mu) \log M(\mu)$ at the critical point $\mu = 1$ using each successive coefficient of the diagonal series for the honeycomb series.

Degree of Polynomial evaluated	Numerical value of polynomial
1	0.07695
2	0.09279
3	0.09057
4	0.08280
5	0.08704
6	0.08729
7	0.08312
8	0.08429
9	0.08376
10	0.08238
11	0.08233
12	0.08194
13	0.08123
14	0.08104
15	0.08062
16	0.08026
17	0.07999
18	0.07968

very conclusively. For all analysis on the magnetization other than the ratio method, 0.0765 is given very consistently and method 4 seems to conclusively rule out $\beta_1 = 1/7$. Also thermodynamics rules out a 1/7, since $1/7 > 1/8 = \beta$. This grouping of the results of the analysis into a 1/7 and a 1/13 is a feature of all the other two dimensional lattices studied. The diagonal series on the three dimensional lattices have a similar but less marked grouping of the results of the analysis.

A possible reason for this contradictory grouping can be found by a study of all the roots to the Padé approximants to the logarithmic derivative of the honeycomb diagonal series. Padé analysis of the logarithmic derivative reveals the pattern of singularities illustrated in Figure 9.5. Note all the non-physical singularities are of the order of unit distance from the origin, and this pattern might affect the ratios very seriously. Also the pole just beyond unity on the real axis shows a very strange behavior. This pole appears to be converging on the point $s = 1$. Through the five highest degree of Padé approximants this pole moves steadily from 1.3 to 1.1, while the location of the physical pole at $s = 1$ stays fixed. This pole has a positive residue that is about an eighth of that of the physical pole but is growing rapidly as the pole

FIGURE 9.5

SINGULARITIES OF THE DIAGONAL SERIES ON THE HONEYCOMB

LATTICE

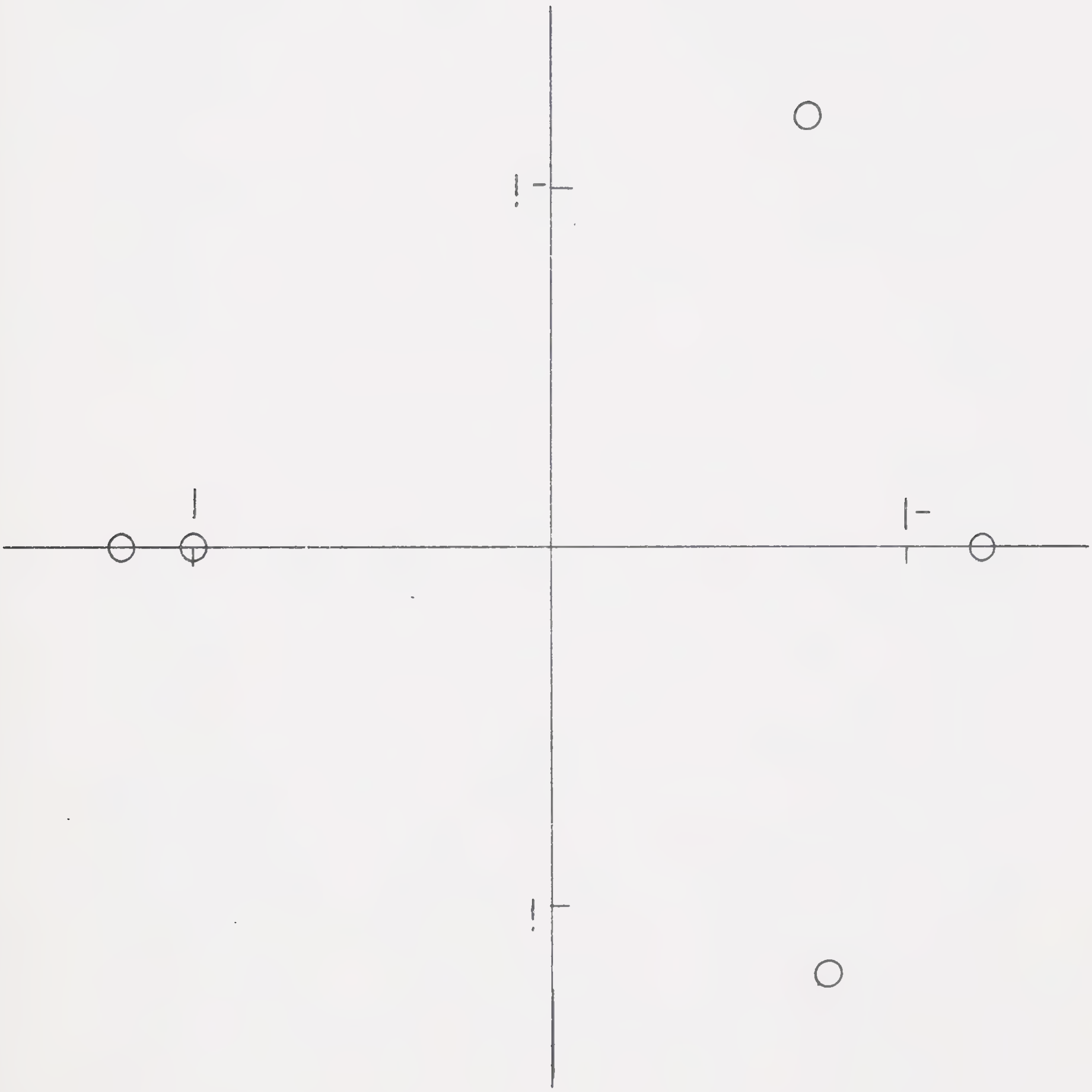

approaches unity. This behavior seems to indicate the presence of two confluent singularities.

Also when the derivative of the diagonal series is multiplied by $(1 - \mu)^{6/7}$ to eliminate the apparent pole at $s = 1$, the analysis shows that there is a very significant singularity still remaining at $s = 1$. This also seems to support the presence of two confluent poles. The grouping of the values of the exponent into two groups can also be explained by the presence of a confluent pole. For example the following function might give the behavior

$$M(\mu) = A((1 - \mu)^{1/15} + 10(1 - \mu)^{1/7}) \quad . \qquad (9.2)$$

The ratios of the series expansion to this function will be dominated in the earlier terms by the exponent $= 1/7$. Since $1/7 >> 1/\delta = 1/15$ the contribution from the 1/7 singularity might totally mask the 1/15 singularity in the derivative but not in the magnetization itself. The occurrence of two confluent singularities has been the assumed behavior of the diagonal series and the value closest to the scaling value has been accepted as the "best" value for the critical exponent. Evidence has been found, on the paths for $p = 3$, 2, 1/2 and 1/3, which indicates the occurrence of a confluent pole for these paths also.

It is thought that the appearance of a confluent singularity might be a general feature of all paths other than the zero field and critical isotherm paths.

CHAPTER 10

FUTURE ANALYSIS

Suitable conformal transformations might sharpen estimates of the critical point and the confidence limits for many of the series. A good choice of a transformation of the series expansion variable will smooth out the ratios and make function (9.1) regular. Transformations of the form

$$s = \mu = \frac{(1 - b)s^*}{1 - bs^*} \tag{10.1}$$

worked well on the diagonal series for the five lattices. As an example the transformation

$$s = \mu = \frac{0.84\ s^*}{1 - 0.16\ s^*} \tag{10.2}$$

has been used on the diagonal series for the square lattice. The ratios become flat and give an estimate of one seventh for the critical exponent. Also, when this transformation is used on the square diagonal series, the evaluation of the series to function (9.1) at the critical point $\mu = 1$ using successively higher coefficients of the series becomes regular as shown in Table 10.1. From this table it can be seen that an upper bound of 0.07964 is very probable. This technique might also be used profitably on the other series analysed.

The paths corresponding to

$$z/z_c \propto \mu^p \tag{10.3}$$

Table 10.1

Value of $(s^*-1)(d/ds^*)\log M(s^*)$ at the critical point $\mu = s^* = 1$ using each successive coefficient of the transformed diagonal series on the square lattice, when $\mu = s = 0.84\, s^*/(1 - 0.16\, s^*)$.

Degree of Polynomial evaluated	Numerical Value of polynomial
7	0.08216
8	0.08957
9	0.08331
10	0.08725
11	0.08348
12	0.08481
13	0.08311
14	0.08355
15	0.08249
16	0.08252
17	0.08190
18	0.08176
19	0.08132
20	0.08111
21	0.08077
22	0.08056
23	0.08029
24	0.08008
25	0.07984
26	0.07964

might also be analysed for small integral values of p and 1/p. Near the critical point these curves become straight lines of slope p. Therefore, according to scaling,these paths should have the same exponent as the diagonal path. The analysis of the series on these paths will give estimates of the critical exponents just above and below the diagonal curve. The preliminary analysis indicates that these paths all have a critical exponent of 1/15 plus or minus 5 %. This gives more validity to the conclusion that scaling theory holds on the diagonal path.

The effect of confluent singularities on the ratios and Padé approximants to truncated series has never been studied in any detail. The conclusions of this thesis show the need for such studies on known functions.

All the analysis completed so far agrees very well with the predictions of scaling theory. Thus one more positive test of the validity of the scaling hypothesis has been added.

APPENDIX

Ising model low temperature magnetization series on paths of the form $z/z_c = 1 - (1 - \mu)^p$ for the honeycomb, square, triangular, hydrogen peroxide, and diamond lattices.

TWO DIMENSIONAL ISING MODEL

SPONTANEOUS MAGNETIZATION COEFFICIENTS

N	HONEYCOMB LATTICE	SQUARE LATTICE	TRIANGULAR LATTICE
0	1.00000000000	1.00000000000	1.00000000000
1	0.0	0.0	0.0
2	0.0	-2.00000000000	0.0
3	-2.00000000000	-8.00000000000	-2.00000000000
4	-6.00000000000	-34.00000000000	0.0
5	-18.00000000000	-152.00000000000	-12.00000000000
6	-54.00000000000	-714.00000000000	2.00000000000
7	-168.00000000000	-3472.00000000000	-78.00000000000
8	-534.00000000000	-17317.99999999999	24.00000000000
9	-1732.00000000000	-88048.00000000000	-548.00000000000
10	-5706.00000000000	-454377.99999999990	228.00000000000
11	-19037.99999999999	-2373047.99999999900	-4050.00000000000
12	-64175.99999999999		2030.00000000000
13	-218189.99999999990		-30959.99999999999
14	-747179.99999999990		17669.99999999999
15	-2574487.99999999900		-242401.99999999990
16	-8918069.99999999900		152519.99999999990

TWO DIMENSIONAL ISING MODEL

LOW TEMPERATURE MAGNETIZATION COEFFICIENTS ON THE PATH Z/ZC=1-(1-U)*1/3

N	HONEYCOMB LATTICE	SQUARE LATTICE	TRIANGULAR LATTICE
0	1.00000000000	1.00000000000	1.00000000000
1	0.0	0.0	0.0
2	0.0	0.0	0.0
3	0.0	-0.17662350914	0.0
4	-0.11542731880	0.17662350914	-0.22222222222
5	0.11542731880	-0.42252014265	0.22222222222
6	-0.31683368465	0.80528093915	-0.07407407407
7	0.55671582343	-1.60434371336	-0.44444444444
8	-1.10855491986	2.72312283741	1.06172839506
9	2.14609407401	-4.14842778666	-1.53086419753
10	-4.20577632245	5.53868061882	1.25102880658
11	8.27732175172	-7.44504966254	-0.09053497942
12	-18.00715628868	13.82438653067	-1.32510288066
13	42.31810485146	-37.22377288341	0.68312757202
14	-101.12459598570	101.25021001950	5.95610425240
15	239.05868118250	-233.52417092350	-23.90672153635
16	-555.91431971310	450.00391119220	57.70187471422
17	1273.35181890400	-772.84198119500	-107.45130315500
18	-2928.56938496000	1377.02914378400	163.08936645840
19	6930.23908220900	-2968.38813822700	-196.49443682370
20	-16950.35913420999	7459.65421316100	143.29506003490
21	42202.11990477999	-19305.46870044999	137.62234754190
22	-105400.55190599990	49101.65174921999	-917.80407232410
23	263016.17230569990	-122972.37323499990	2566.56188363300
24	-658045.35722869990	302007.82946719990	-5146.63855818400
25	1658342.02325799900	-716860.11281629990	7084.34474193700
26	-4219159.42784899900	1637081.41000999900	-2235.62766390500
27	10834910.75830999000	-3642601.99194399900	-24522.44409695999
28	-28048819.28788999000		
29	73088901.68262999000		
30	-191442261.38339990000		
31	503645472.55229990000		
32	-1331018868.93699900000		
33	3536037878.99799900000		
34	-9445720895.55499700000		
35	25357034927.72999000000		
36	-68353862403.94999000000		
37	184967041737.39990000000		
38	-502571567938.59990000000		
39	1371546952199.99900000000		

TWO DIMENSIONAL ISING MODEL

LOW TEMPERATURE MAGNETIZATION COEFFICIENTS ON THE PATH Z/ZC=1-(1-U)*1/2

N	HONEYCOMB LATTICE	SQUARE LATTICE	TRIANGULAR LATTICE
0	1.00000000000	1.00000000000	1.00000000000
1	0.0	0.0	0.0
2	0.0	0.0	0.0
3	0.0	-0.11774900609	0.0
4	-0.07695154587	0.05887450305	-0.14814814815
5	0.03847577293	-0.16162028427	0.07407407407
6	-0.12371462743	0.19628235536	0.0
7	0.12371462743	-0.32463405399	-0.19753086420
8	-0.21798098310	0.38628102507	0.27434842250
9	0.28650002978	-0.49181729620	-0.25788751715
10	-0.43497690491	0.55146127750	0.01920438957
11	0.62381423713	-0.73114699053	0.24142661180
12	-1.06597278936	1.10711494191	-0.39099730732
13	1.78847082248	-1.90613183588	0.13971447442
14	-3.02993085723	3.08370638717	0.51597825535
15	5.06058850807	-4.55759655328	-1.44063404969
16	-8.36985852740	6.21900600668	2.10681524384
17	13.73238720981	-8.58886360759	-2.01312281137
18	-23.20554763451	12.83612670166	0.82421190687
19	40.42937264964	-20.71654983815	1.15800499648
20	-71.26135680788	34.23905708722	-3.21170149057
21	125.43971709120	-56.63691207608	4.38722238565
22	-220.65287790970	93.57549614217	-4.08624963560
23	389.24920032960	-153.64618885810	1.98481152606
24	-691.43519552000	248.22885100680	2.37798747913
25	1238.71969590800	-395.68422592160	-10.64836229144
26	-2235.65010304800	631.24342466920	25.51496672650
27	4057.24993376900	-1016.71039231900	-47.95837470537
28	-7393.72293050100		
29	13516.25494310999		
30	-24784.26157800999		
31	45630.14817147999		
32	-84411.82781071998		
33	156815.74118039990		
34	-292233.10657119990		
35	546057.21855099990		
36	-1023468.43729299900		
37	1924863.90227899900		
38	-3632193.02821999900		
39	6874041.27622399900		

TWO DIMENSIONAL ISING MODEL

LOW TEMPERATURE MAGNETIZATION COEFFICIENTS ON THE PATH Z/ZC=1-(1-U)*1

N	HONEYCOMB LATTICE	SQUARE LATTICE	TRIANGULAR LATTICE
0	1.00000000000	1.00000000000	1.00000000000
1	0.0	0.0	0.0
2	-0.03847577293	0.0	0.0
3	-0.03092865686	-0.05887450305	0.0
4	-0.02190115568	0.0	-0.07407407407
5	-0.01537037354	-0.04040507107	0.0
6	-0.01316682878	0.00866551777	0.0
7	-0.01115535668	-0.03119586398	-0.04938271605
8	-0.00909805507	0.00734055666	0.01920438957
9	-0.00810585442	-0.02299100828	-0.01646090535
10	-0.00717550250	0.00545191139	-0.02469135802
11	-0.00634061512	-0.01866861501	0.01646090535
12	-0.00576157571	0.00557615102	-0.02052532642
13	-0.00525359903	-0.01638577584	-0.01117715795
14	-0.00479797106	0.00521855008	0.01351420007
15	-0.00444055845	-0.01406357916	-0.02458974750
16	-0.00411583707	0.00463274539	0.00269832399
17	-0.00383469084	-0.01240580064	0.00344723121
18	-0.00359145668	0.00434155577	-0.02018662467
19	-0.00337278413	-0.01118919470	0.00891663734
20		0.00410798538	-0.00495954152
21		-0.01019097730	-0.01316755346
22		0.00386124020	0.01007547125
23		-0.00932591190	-0.01079134460
24		0.00364096970	-0.00517113590
25		-0.00861686438	0.00686686449
26		0.00345506799	-0.01237773978
27		-0.00800772338	0.00076399676

TWO DIMENSIONAL ISING MODEL

LOW TEMPERATURE MAGNETIZATION COEFFICIENTS ON THE PATH Z/ZC=1-(1-U)*2

N	HONEYCOMB LATTICE	SQUARE LATTICE	TRIANGULAR LATTICE
0	1.00000000000	1.00000000000	1.00000000000
1	0.0	0.0	0.0
2	0.0	0.0	0.0
3	0.0	-0.23549801218	0.0
4	-0.30780618347	0.23549801218	-0.59259259259
5	0.46170927520	-0.38211507158	0.88888888889
6	-0.72571314732	0.62350913716	-0.44444444444
7	1.02819279236	-1.01886081879	-1.50617283951
8	-1.34838009968	1.59246158555	5.17969821673
9	1.66791544605	-2.52434722066	-8.69135802469
10	-1.95028063878	3.97964152616	6.58436213992
11	2.10098093846	-6.36292171669	9.16323731138
12	-2.17530667833	10.23670919542	-42.69735304578
13	2.00657346344	-16.61527337016	79.57770665041
14	-1.37457937620	27.05692026716	-69.74414469339
15	-0.06677093360	-44.21260909871	-71.50190519738
16	2.81635812713	72.39792500174	406.00954009950
17	-7.56876025819	-118.85753469320	-826.51510515750
18	14.86023660111	195.56410873530	856.72048637570
19	-25.25550884362	-322.49956499840	403.25385257570
20	39.34232558200	532.87193204010	-3778.52275159400
21	-57.53791608374	-882.08031821660	8535.90980497700
22	79.70007962586	1462.47349253500	-10098.91519653999
23	-104.78580889340	-2428.29351976200	-1155.30672029600
24	129.70383380030	4037.27507533900	35648.15299607999
25	-148.05016778940	-6720.60299623300	-89517.56607899999
26	148.87107538390	11200.08246129999	118749.44843229990
27	-115.26708226710	-18685.02289479999	-20238.03828456999
28	22.44988927281		
29	163.91932594220		
30	-489.17564568360		
31	1009.88203100900		
32	-1790.75317021200		
33	2895.57468069100		
34	-4369.96577068600		
35	6211.89493603800		
36	-8325.32260096200		
37	10451.97403842999		
38	-12075.53483565999		
39	12292.72961406999		

TWO DIMENSIONAL ISING MODEL

LOW TEMPERATURE MAGNETIZATION COEFFICIENTS ON THE PATH Z/ZC=1-(1-U)*3

N	HONEYCOMB LATTICE	SQUARE LATTICE	TRIANGULAR LATTICE
0	1.00000000000	1.00000000000	1.00000000000
1	0.0	0.0	0.0
2	0.0	0.0	0.0
3	0.0	-0.52987052741	0.0
4	-1.03884586921	1.05974105482	-2.00000000000
5	3.11653760763	-1.97405446449	6.00000000000
6	-6.66060468227	4.32796471423	-8.00000000000
7	13.13742242937	-9.75711491882	-6.00000000000
8	-23.63979650858	21.43439461418	71.33333333333
9	37.64488266881	-47.05118795410	-235.33333333330
10	-51.42285019775	103.58725086320	455.92592592590
11	91.29223839643	-229.15967025970	-283.33333333330
12	-2.72877343243	509.53651185840	-1738.66666666700
13	-169.93679156840	-1138.70348542300	8356.22222222200
14	622.21966800620	2555.56489288000	-20861.40740740999
15	-1650.44307091800	-5755.42880922300	26623.48148147999
16	3766.64891472600	12999.72514763999	31611.77777777999
17	-7750.60329102300	-29437.06718706999	-294242.93827159990
18	14537.48027722999	66809.84840528998	934872.71604939990
19	-24570.57038278999	-151942.36747509990	-1713639.67901199900
20	35817.63072874999	346202.56600639990	559970.01920439990
21	-38851.62953097999	-790178.02243279990	9032126.94650199900
22	6051.10685609800	1806343.69585799900	-38855830.41974999000
23	129835.41740859990	-4135238.28839699900	92114760.78188999000
24	-514064.87032639990	9479280.69431299900	-103364358.08229990000
25	1430302.67940199900	-21756076.21167999000	-205092860.27429990000
26	-3377082.68321499900	49989271.25380999000	1487830796.42199900000
27	7116663.76006099900	-114981806.04639990000	-4466565875.56899800000
28	-13553483.48577999000		
29	23073165.87977999000		
30	-33508673.05154999000		
31	35039789.63143999000		
32	1077491.72173699900		
33	-144961014.32069990000		
34	548317878.68909990000		
35	-1507303804.57199900000		
36	3539939687.08499900000		
37	-7427227603.24899800000		
38	14055876626.30999000000		
39	-23648179780.56999000000		

TWO DIMENSIONAL ISING MODEL

COEFFICIENTS FOR THE MAGNETIZATION ON THE CRITICAL ISOTHERM

N	HONEYCOMB LATTICE	SQUARE LATTICE	TRIANGULAR LATTICE
0	1.00000000000	1.00000000000	1.00000000000
1	-0.03847577293	-0.05887450305	-0.07407407407
2	-0.02756788665	-0.03173955329	-0.03017832647
3	-0.01977746305	-0.01850444507	-0.01961083168
4	-0.01430254895	-0.01481347971	-0.01450772522
5	-0.01060322332	-0.01125167470	-0.01144630737
6	-0.00945291753	-0.00963314220	-0.00939115536
7	-0.00828699552	-0.00795813087	-0.00797401315
8	-0.00714710905	-0.00702779131	-0.00691849428
9	-0.00611784478	-0.00615916156	-0.00609679003
10	-0.00560346789	-0.00551978309	-0.00544981546
11	-0.00511791695	-0.00498635603	
12	-0.00463123684	-0.00455197995	
13	-0.00423750346	-0.00417341609	
14	-0.00394796240	-0.00386297893	
15	-0.00366889007	-0.00358759394	
16	-0.00342227244		
17	-0.00321170856		
18	-0.00302424934		
19	-0.00285704732		
20	-0.00270688018		
21	-0.00256851207		

THREE DIMENSIONAL ISING MODEL

SPONTANEOUS MAGNETIZATION COEFFICIENTS

N	HYDROGEN PEROXIDE LATTICE	DIAMOND LATTICE
0	1.00000000000	1.00000000000
1	0.0	0.0
2	0.0	-2.00000000000
3	-2.00000000000	-8.00000000000
4	-6.00000000000	-26.0000000000
5	-18.0000000000	-80.0000000000
6	-48.0000000000	-268.000000000
7	-126.000000000	-944.000000000
8	-324.000000000	-3474.00000000
9	-830.000000000	-13071.9999999
10	-2154.00000000	-49671.9999999
11	-5784.00000000	-191271.999999990
12	-16145.9999999	-744499.999999990
13	-46301.9999999	-2924679.99999900
14	-134081.99999990	-11596283.9999999000
15	-387723.99999990	-46364455.9999999000
16	-1117163.99999900	

THREE DIMENSIONAL ISING MODEL

LOW TEMPERATURE MAGNETIZATION COEFFICIENTS ON THE PATH Z/ZC=1-(1-U)*1/3

N	HYDROGEN PEROXIDE LATTICE	DIAMOND LATTICE
0	1.00000000000	1.00000000000
1	0.0	0.0
2	0.0	0.0
3	0.0	-0.31144514539
4	-0.19183692300	0.31144514539
5	0.19183692300	-0.95530194590
6	-0.61193024786	1.94546899134
7	1.09596921373	-4.52308334383
8	-2.40502985698	10.41980972134
9	4.91409241790	-24.49095434633
10	-10.36343625347	58.20324440392
11	21.77564486783	-139.81320200530
12	-46.16427169915	336.34657406330
13	98.24889537253	-809.31814923150
14	-210.21680403570	1946.93991031000
15	451.69517646440	-4680.93121853300
16	-974.61802322070	11241.87921997999
17	2110.75428755200	-26970.33267467999
18	-4587.16589842100	64651.15935865999
19	10000.62210519999	-154887.08543349990
20	-21884.97506036999	370961.44700069990
21	48124.97720948999	-888517.87419819990
22	-106433.81447139990	2128957.56958799900
23	236826.94697029990	-5104480.04902599900
24	-530125.44031359990	12249721.70028999000
25	1193270.90668399900	-29429284.57753999000
26	-2699494.02859699900	70790325.57653999000
27	6134877.99802999900	-170507425.18579990000
28	-14000951.20312999000	411243012.29239990000
29	32078671.38830999000	-993184098.20109990000
30	-73767738.59631999000	2401654746.06399900000
31	170209606.35529990000	-5814383518.44199800000
32	-393951031.80249980000	14091791752.78999000000
33	914380496.28939990000	-34186428962.87999000000
34	-2127907818.81999900000	
35	4964417676.22899800000	
36	-11610438901.21999000000	
37	27219589444.46999000000	
38	-63966758811.06999000000	
39	150676912599.49990000000	

THREE DIMENSIONAL ISING MODEL

LOW TEMPERATURE MAGNETIZATION COEFFICIENTS ON THE PATH Z/ZC=1-(1-U)*1/2

N	HYDROGEN PEROXIDE LATTICE	DIAMOND LATTICE
0	1.00000000000	1.00000000000
1	0.0	0.0
2	0.0	0.0
3	0.0	-0.20763009693
4	-0.12789128200	0.10381504846
5	0.06394564100	-0.37843862108
6	-0.24354871416	0.48621426396
7	0.24354871416	-0.97836992684
8	-0.49197481524	1.66237233921
9	0.66298763505	-3.08719129463
10	-1.11545308037	5.64103241883
11	1.67961979915	-10.53239534505
12	-2.70272716673	19.54888206675
13	4.23778054314	-36.49631388640
14	-6.78658519114	68.12568093419
15	10.83102518030	-127.35302440440
16	-17.43254862345	238.07238011320
17	28.11057741373	-445.38540233100
18	-45.54313841226	833.61314060820
19	73.99434499636	-1561.34520323600
20	-120.94281121190	2926.80284590600
21	198.76568662570	-5491.92806553700
22	-328.66060635980	10316.40422730999
23	546.37540168220	-19402.20679461999
24	-912.76699711790	36536.11987722999
25	1531.23371436800	-68889.79457023998
26	-2578.46963684100	130061.07190019990
27	4356.87244989600	-245861.17435399990
28	-7385.13413768400	465332.32179919990
29	12554.04680933999	-881741.71962359990
30	-21395.85936754999	1672614.27772699900
31	36549.56961655999	-3176118.25298499900
32	-62569.15527401999	6036902.92969599900
33	107328.67608509990	-11484708.03164999000
34	-184469.31454389990	
35	317664.85217059990	
36	-548065.45634329990	
37	947301.38185619990	
38	-1640233.92138099900	
39	2844821.47743299900	

THREE DIMENSIONAL ISING MODEL

LOW TEMPERATURE MAGNETIZATION COEFFICIENTS ON THE PATH Z/ZC=1-(1-U)*1

N	HYDROGEN PEROXIDE LATTICE	DIAMOND LATTICE
0	1.00000000000	1.00000000000
1	0.0	0.0
2	-0.06394564100	0.0
3	-0.06088717854	-0.10381504846
4	-0.04979690958	0.0
5	-0.03972601657	-0.09460965527
6	-0.03183969494	0.02694391072
7	-0.02585376113	-0.09699807859
8	-0.02130803823	0.05893143568
9	-0.01781712962	-0.11671223395
10	-0.01540770921	0.10181747565
11	-0.01371631626	-0.15837152464
12	-0.01237820992	0.16288189325
13	-0.01124689954	-0.22793744766
14	-0.01026028791	0.25554272151
15	-0.00938903803	-0.33873741234
16	-0.00863565604	0.39812428234
17	-0.00799446299	-0.51355608836
18	-0.00744197774	0.61995986957
19	-0.00695755442	-0.78903760434
20		0.96810624387
21		-1.22448806494
22		1.51797145211
23		-1.91563003265
24		2.39125104167
25		-3.01697843905
26		3.78458301152
27		-4.77862378941
28		6.01634813527
29		-7.60602051174
30		9.60322210944
31		-12.15778802075
32		15.38527293150
33		-19.50584542451

THREE DIMENSIONAL ISING MODEL

LOW TEMPERATURE MAGNETIZATION COEFFICIENTS ON THE PATH Z/ZC=1-(1-U)*2

N	HYDROGEN PEROXIDE LATTICE	DIAMOND LATTICE
0	1.00000000000	1.00000000000
1	0.0	0.0
2	0.0	0.0
3	0.0	-0.41526019385
4	-0.51156512799	0.41526019385
5	0.76734769198	-0.86069229063
6	-1.35786870264	1.56641843475
7	2.01233535430	-2.98183233200
8	-2.79309451149	5.73100796912
9	3.55490411444	-11.27029210573
10	-4.15729134246	22.34192262700
11	4.15262371469	-44.85374961388
12	-3.04785925957	90.56296622680
13	-0.13819731089	-183.97664879920
14	6.59045149799	375.44758266080
15	-18.03929153950	-769.24840251890
16	36.43518692851	1581.19712586200
17	-63.94003026987	-3259.45428730200
18	102.16542431090	6735.64971052600
19	-151.29942898500	-13950.08738634999
20	207.77321375840	28949.51306347999
21	-261.49725418870	-60186.22254246999
22	291.58988908870	125337.02370489990
23	-260.99350048680	-261416.82557489990
24	109.83959597830	546024.24654379990
25	251.42370537830	-1142017.21182999900
26	-949.09879685890	2391543.01723799900
27	2150.39385100900	-5014120.71873399900
28	-4060.97273448600	10524262.81345990000
29	5907.90536450503	-22112[illegible]52999000
30	-10895.02326770999	46506782.92196999000
31	16108.24396998999	-97902641.53653999000
32	-22338.26239804999	206278112.12019990000
33	28771.30530647999	-434982882.96699990000
34	-33481.10231631999	
35	32639.12191998999	
36	-19358.00344538999	
37	-17886.74806580999	
38	97206.16945281998	
39	-245334.84688169990	

THREE DIMENSIONAL ISING MODEL

LOW TEMPERATURE MAGNETIZATION COEFFICIENTS ON THE PATH Z/ZC=1-(1-U)*3

N	HYDROGEN PEROXIDE LATTICE	DIAMOND LATTICE
0	1.00000000000	1.00000000000
1	0.0	0.0
2	0.0	0.0
3	0.0	-0.93433543617
4	-1.72653230696	1.86867087234
5	5.17959692088	-4.11168641926
6	-11.83799068964	10.46872913592
7	24.90704276806	-26.90832925603
8	-46.59512441540	69.41578137656
9	74.69906128086	-182.65946412500
10	-94.43442662529	486.56695828620
11	51.26923863174	-1309.01390833300
12	2[illegible]2.4816879846[illegible]	3549.91293911100
13	-1[illegible]9.[illegible]2430[illegible]	-[illegible].4[illegible]9443[illegible]
14	3083.18078049000	26579.8[illegible]30831[illegible]99
15	-7733.62862087000	-73241.23105344999
16	17012.72223436999	202572.23545269990
17	-33248.52272762999	-562077.15192439990
18	56536.34016343999	1563956.01689899900
19	-76734.34621502998	-4362375.39874199900
20	52587.50146339999	12194824.03176999000
21	136061.09190879990	-34157561.58119999000
22	-785843.14250849990	95846822.51863998000
23	2545179.54183699900	-269389776.27029990000
24	-6675281.96059699900	758297566.18459990000
25	15299842.77268999000	-2137488060.86699900000
26	-31212448.96640999000	6032950056.67399800000
27	55938826.82149999000	-17048231160.71999000000
28	-82749571.75454999000	48230107353.64999000000
29	77208976.46773999000	-136588987864.39990000000
30	69618500.01942999000	387207641179.29990000000
31	-641529508.43029990000	-1098696380761.99900000000
32	2288909578.02599900000	3120283040166.99900000000
33	-6343934286.48899800000	-8868940125194.99900000000
34	15213677122.78999000000	
35	-32513117143.37999000000	
36	61762859473.20999000000	
37	-100409068665.59990000000	
38	121360791699.19990000000	
39	-252135734 85.51999000000	

THREE DIMENSIONAL ISING MODEL

COEFFICIENTS FOR THE MAGNETIZATION ON THE CRITICAL ISCTHERM

N	HYDROGEN PEROXIDE LATTICE	DIAMOND LATTICE
0	1.00000000000	1.00000000000
1	-0.06394564100	-0.10381504846
2	-0.05270908854	-0.06766574455
3	-0.04169639999	-0.04673791144
4	-0.03346993969	-0.03423051922
5	-0.02740650289	-0.02620259429
6	-0.02285699723	-0.02144837062
7	-0.01936709634	-0.01807433522
8	-0.01663323930	-0.01553902655
9	-0.01445111132	-0.01358629560
10	-0.01278806245	-0.01206995168
11	-0.01148493064	-0.01083201572
12	-0.01042430507	-0.00980618843
13	-0.00953376547	-0.00894954194
14	-0.00877597713	-0.00822253334
15	-0.00812049154	-0.00759615333
16	-0.00754709981	-0.00705223947
17	-0.00704253119	-0.00657637012
18	-0.00659722596	
19	-0.00620183219	
20	-0.00584829637	
21	-0.00553028892	

0
41 13.636 RC=0

REFERENCES

Ahlers, G., 1969. Phys. Rev. Lett. 23, 464.

Ahlers, G., 1972. (Private communication to Dr. D.D. Betts).

Baker, G.A. Jr., 1961. Phys. Rev. 124, 768.

Baker, G.A. Jr., 1965. Advances in Theoretical Physics I, Ed. K.A. Brueckner (New York Academic Press).

Baker, G.A. Jr., 1968. J. Appl. Phys. 39, 616.

Baker, G.A. Jr., Gammel, J.L., Wills, J.G., 1961. J. Math. Anal. Appl. 2, 405.

Betts, D.D., 1973 (to be published).

Betts, D.D., Elliott, C.J., Ditzian, R.V., 1968. Can. J. Phys. 46, 971.

Betts, D.D. and Lee, M.H., 1968. Phys. Rev. Lett. 20, 1507.

Betts, D.D., Elliott, C.J., Lee, M.H., 1969. Phys. Lett. 29A, 150.

Betts, D.D., Elliott, C.J., Lee, M.H., 1970. Can. J. Phys. 48, 1566.

Betts, D.D., Guttmann, A.J. and Joyce, G.S., 1971. J. Phys. C. 4, 1994.

Betts, D.D., Filipow, L., 1972 (to be published).

Buckingham, M.J. and Gunton, J.D., 1968. Phys. Rev. 178, 848.

Cooke et al, 1972. J. de Phys. Supp., C1 - 643.

Domb, C., 1960. Advanc. Phys. 9, Nos. 34, 35.

Domb, C. and Sykes, M.F., 1957a. Proc. Roy. Soc. A. 240, 214.

Domb, C. and Sykes, M.F., 1957b. Phys. Rev. 108, 1415.

Domb, C. and Hunter, D.L., 1965. Proc. Phys. Soc. 86, 1147.

Essam, J.W. and Fisher, M.E., 1963. J. Chem. Phys. 38, 802.

Essam, J.W. and Sykes, M.F., 1963. Physica 29, 378.

Essam, J.W. and Hunter, D.L., 1968. Proc. Phys. Soc. 1, 392.

Fisher, M.E., 1967. Rep. Prog. Phys. XXX, 615.

Fisher, M.E., 1969. Phys. Rev. 180, 594.

Gaunt, D.S., 1967. Proc. Phys. Soc. 92, 150.

Gaunt, D.S. and Domb, C., 1970. J. Phys. C. 3, 1442.

Gaunt, D.S. and Guttmann, A.J., 1973. "Series Expansion: Analysis of Coefficients" (to be published).

Gibberd, R.W., 1970. Can. J. Phys. 48, 307.

Griffiths, R.B., 1965. Phys. Rev. Lett. 14, 623.

Griffiths, R.B., 1967. J. Math. Phys. 8, 478, 484.

Griffiths, R.B., 1972. (Private communication to Dr. D.D. Betts).

Huiskamp, W.J., 1972. (To be published in L.T.P. 13).

Hunter, D.L., 1968. J. Phys. C. 1969. 2, 941.

Kadanoff, L.P. et al, 1967. Rev. Mod. Phys. 39, 395-431.

Kelly, D.G. and Sherman, S., 1968. J. Math. Phys. 9, 466.

Leu, J.A., Betts, D.D., Elliott, C.J., 1969. Can. J. Phys. 47, 1671.

Matsubara, I. and Matsuda, H., 1956. Prog. Theor. Phys. (Kyoto) 16, 416.

Oitmaa, J. and Elliott, C.J., 1970. Can. J. Phys. 48, 2383.

Patashinskii, A.Z. and Pokrovskii, V.L., 1966. Soviet Physics JETP, 23, 292.

Rushbrooke, G.S., 1963. J. Chem. Phys. 39, 842.

Stanley, H.E., 1971. Introduction to Phase Transitions and Critical Phenomena (Clarendon, Oxford).

Stephenson, J., 1971. Physical Chemistry 8B, 717.

Sykes, M.F., Essam, J.W. and Gaunt, D.S., 1965. J. Math. Phys. 6, 283.

Sykes, M.F., Essam, J.W., Heap, B.R. and Hiley, B.J., 1966. J. Math. Phys. 7, 1557.

Sykes, M.F., Martin, J.L. and Hunter, D.L., 1967. Proc. Phys. Soc. 91, 671.

Sykes, M.F., Wyles, J.A., 1972a. J. Phys. A: Gen. Phys. 5, 640.

Sykes, M.F. et al, 1972b. J. Phys. A: Gen. Phys. 5, 667.

Sykes, M.F. et al, 1973. J. Math. Phys. (in press).

van der Waerden, B.L., 1941. Z. Phys. 118, 473.

Vicentini-Missoni, M., Levelt-Sengers, J.M.H. and Green, M.S., 1969. J. Res. N.B.S. 73A, 563.

Watson, P.G., 1969. J. Phys. C: Solid St. Phys. 2, 1883-1885.

Widom, B., 1965a. J. Chem. Phys. 43, 3892.

Wodom, B., 1965b. J. Chem. Phys. 43, 3898.

Wortis, M., 1969. (Private communication to Dr. D.D. Betts).